

WT1 Peptide Vaccine Stabilized Intractable Ovarian Cancer Patient for One Year: A Case Report

SATOSHI DOHI¹, SATOSHI OHNO^{1,2}, YUMIKO OHNO¹, MASAHIRO TAKAKURA¹,
SATORU KYO¹, GEN-ICHIRO SOMA^{3,4}, HARUO SUGIYAMA⁵ and MASAKI INOUE¹

¹Department of Obstetrics and Gynecology, Kanazawa University,
Graduate School of Medical Science, Ishikawa, Japan;

²Consolidated Research Institute for Advanced Science and Medical Care, Waseda University, Tokyo, Japan;

³Institute for Health Sciences, Tokushima Bunri University, Tokushima, Japan;

⁴Center for Drug Delivery Research, Tokyo University of Science, Chiba, Japan;

⁵Department of Functional Diagnostic Science, Osaka University Graduate School of Medicine, Osaka, Japan

Abstract. We report on Wilms tumor (WT1) peptide immunotherapy in a patient with intractable ovarian cancer patient over an extended period. Case Report: Immunotherapy using WT1 peptide has been undergoing clinical trials for gynecological cancer. We used WT1 peptide vaccination to treat a 53-year-old woman suffering from ovarian cancer with peritoneal dissemination. After 2 months, her pleural and cardiac effusion had disappeared, and the sum of the longest diameter of the target lesion (in the pelvic mass) was reduced. There was a weak positive correlation between CA125 and mononuclear phagocyte/lymphocyte ratio (Spearman's $\rho=0.275$, $p=0.015$). Intradermally administered WT1 peptide vaccination in a case of intractable ovarian cancer stabilized the disease over the course of one year. However, the immunotherapeutic mechanism of WT1 peptide and immunological escape mechanism for carcinoma cells remain to be elucidated.

Ovarian cancer is one of the most common gynecological malignancies in Japan. Its frequency has dramatically increased in the last decade. Although there are well-established surgical and chemotherapeutic treatments, the need for molecular-target therapy has increased, especially for recurrent disease that has acquired radio- or chemoresistance.

Correspondence to: Satoshi Dohi, Department of Obstetrics and Gynecology, Kanazawa University, Graduate School of Medical Science, 13-1 Takaramachi, Kanazawa, Ishikawa, 920-8640 Japan. Tel: +81 762652425, Fax: +81 762344266, e-mail: satoshi.dohi1018@gmail.com

Key Words: WT1 peptide vaccine, immunotherapy, ovarian cancer.

The Wilms' tumor gene *WT1* has been isolated and identified as a gene responsible for a childhood renal neoplasm, Wilms' tumor (1-3). This gene encodes a zinc finger transcription factor and plays important roles in cell growth and differentiation (4, 5). Although *WT1* was first categorized as a tumor-suppressing gene, it was recently demonstrated that the wild-type *WT1* possessed an oncogenic rather than tumor-suppressing function in many kinds of malignancies (6). *WT1* is highly expressed in hematological malignancies and solid tumors, including ovarian cancer (7, 8).

WT1 is now regarded as a molecular target for immunotherapy in various malignant tumor types. Clinical trials of *WT1* peptide-based cancer immunotherapy are ongoing: *WT1* peptide vaccination has been shown to be safe and clearly effective against several kinds of malignancies (9-13).

Ohno *et al.* reported that twelve patients with *WT1*/human leukocyte antigen (HLA)-A*2402-positive gynecological cancer were included in a phase II clinical trial of *WT1* vaccine therapy. This study evaluated clinical response after a *WT1* vaccine was administered 12 times over three months and found that *WT1* vaccine therapy for patients with gynecological cancer was safe and produced clinical responses: stable disease (SD) in 3 patients and progressive disease (PD) in 9 patients (13).

In the following study, we report a case of intractable ovarian cancer in which an intradermally administered *WT1* peptide vaccination stabilized the disease over the course of a year.

Clinical study. This case report concerns a patient from our *WT1* peptide vaccination study. Entry criteria for the study were as follows: 16-79 years of age, immunohistochemical expression of *WT1* in cancer cells of more than 3 months, performance status 0-1, no severe organ function impairment and the written informed consent of the patient. At least 4

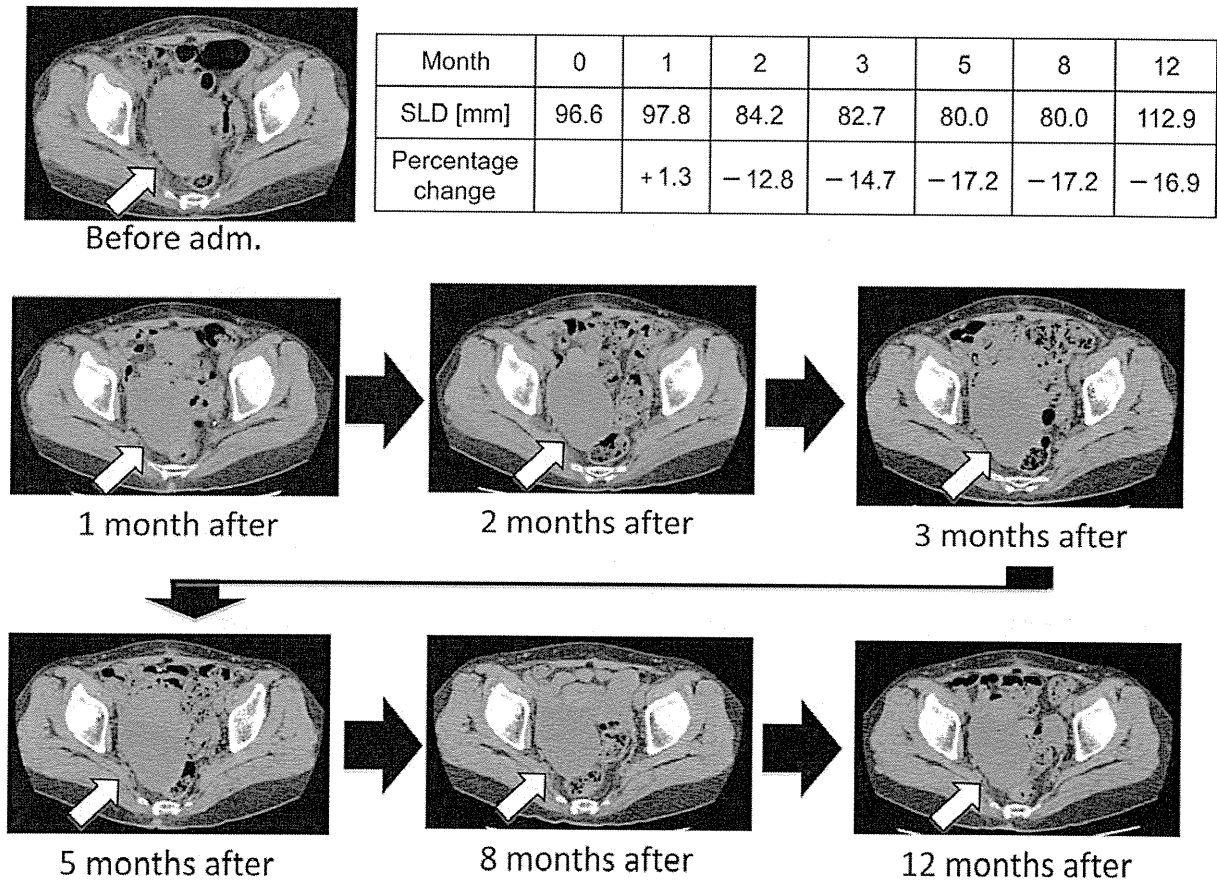


Figure 1. Computed tomography of the patient before, during and after treatment. White arrows indicate primary tumor mass. SLD, Sum of the longest diameters.

weeks prior to immunotherapy, the patient had to be free from antitumor treatments such as surgery, chemotherapy and radiotherapy. The protocol was approved by the Institutional Review Board and the Ethical Committee at Kanazawa University.

WT1 peptide treatment plan. The WT1 peptide vaccine consists of an HLA-A*2402-restricted, modified 9-mer WT1 peptide (amino acids 235-243 CYTWNQMNL), in which Y is substituted for M at amino acid position 2 (the anchor position) of the natural WT1 peptide. The WT1 peptide [Good Manufacturing Practice (GMP) grade] was purchased from Multiple Peptide Systems (San Diego, CA, USA) as lyophilized peptide.

Patients received intradermal injections of 3.0 mg HLA-A*2402-restricted adjuvant (EPPIC S.A., Paris, France). Vaccinations were scheduled weekly for 12 consecutive weeks (13). Efficacy was based on computed tomography (CT) obtained at baseline and after 4, 8 and 12 weeks exposure to the vaccine.

Case Report

A 53-year-old woman was diagnosed as having serous ovarian adenocarcinoma in November 2007. After omentectomy of a pelvic mass with peritoneal dissemination, tri-weekly combination chemotherapy with paclitaxel and carboplatin produced SD and tumor shrinkage of 25%. This was followed by weekly administration of docetaxel, which also contributed to SD.

The patient participated in our WT1 vaccine trial beginning in October 2008. She received HLA-A*2402, and met the inclusion criteria for the phase II clinical study. She was administered WT1 at weekly intervals.

Decrease in tumor size and normalization of tumor marker (CA125). According to the internationally approved Response Evaluation Criteria in Solid Tumors (RECIST) guidelines, sum of the longest diameter (SLD) of the target (pelvic) lesion was reduced: the length was 96.5 mm before administration, 97.8 mm (+1.3%) after 1 month, 84.2 mm (-12.8%) after 2 months,

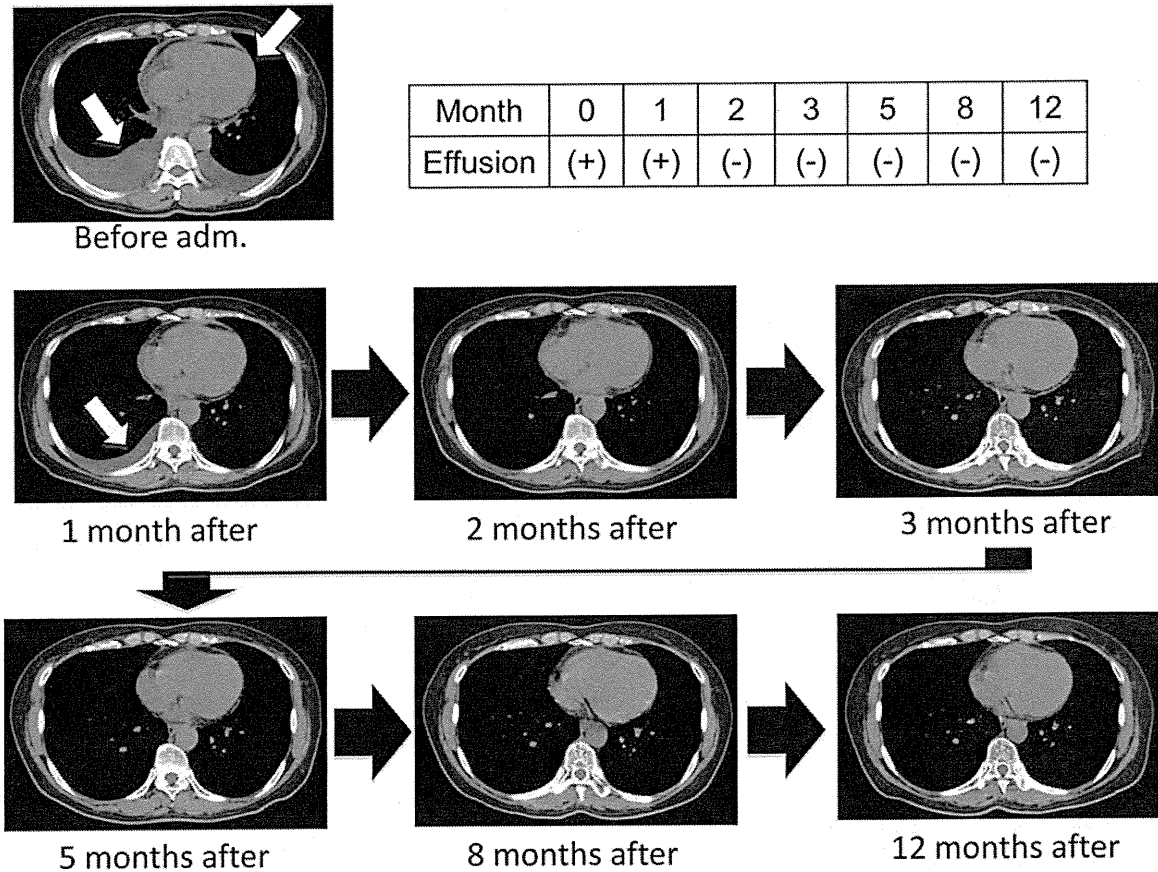


Figure 2. Computed tomography of the patient before, during and after treatment. White arrows indicate pleural and cardiac effusion.

and 82.7 mm after 3 months (-14.7%); after 3 months' administration, SLD continued to decrease (Figure 1). In addition, pleural and cardiac effusions disappeared within two months of beginning administration, and remained absent (Figure 2). Dosage of vaccine was increased from 41 units/ml to 160 units/ml after 1 month of administration, and the level of CA125 normalized after 3 months. According to the patient's wishes, we continued to administer the vaccine, with concomitant normalization/suppression of CA125 (Figure 3a).

No adverse effects of vaccination were observed other than a local inflammatory response with erythema at the injection sites.

Mononuclear phagocyte/lymphocyte ratio (Mo/Ly ratio) and CA125. To evaluate the immunological response to WT1 peptide vaccination, we analyzed the correlation between CA125 and the Mo/Ly ratio (Figure 3b). A weak positive correlation was observed (Spearman's $\rho=0.275$, $p=0.015$).

Although WT1 peptide vaccination was continued for one year, CA125 began to gradually increase approximately 9

months following initial administration (Figure 3a). The patient subsequently dropped out of the clinical trial due to receiving another newly approved chemotherapy regimen for ovarian cancer.

Discussion

Ovarian cancer is a common malignant gynecological cancer of perimenopausal women. Patients with metastatic disease have a poor prognosis, with 5-year progression-free survival usually less than 30% in Japan.

Our patient had primary disease in the ovary, with metastases in the uterus, peritoneum, pelvic lymph nodes and omental. She also developed a pelvic mass with ascites and pleural effusion during chemotherapy, indicating poor response to chemotherapy. Because of her poor prognosis, she was selected for WT1 peptide immunotherapy. Immediately following inception of peptide immunotherapy, the size of the pelvic mass increased, but within two months, a decrease in tumor size and normalization of the level of tumor marker

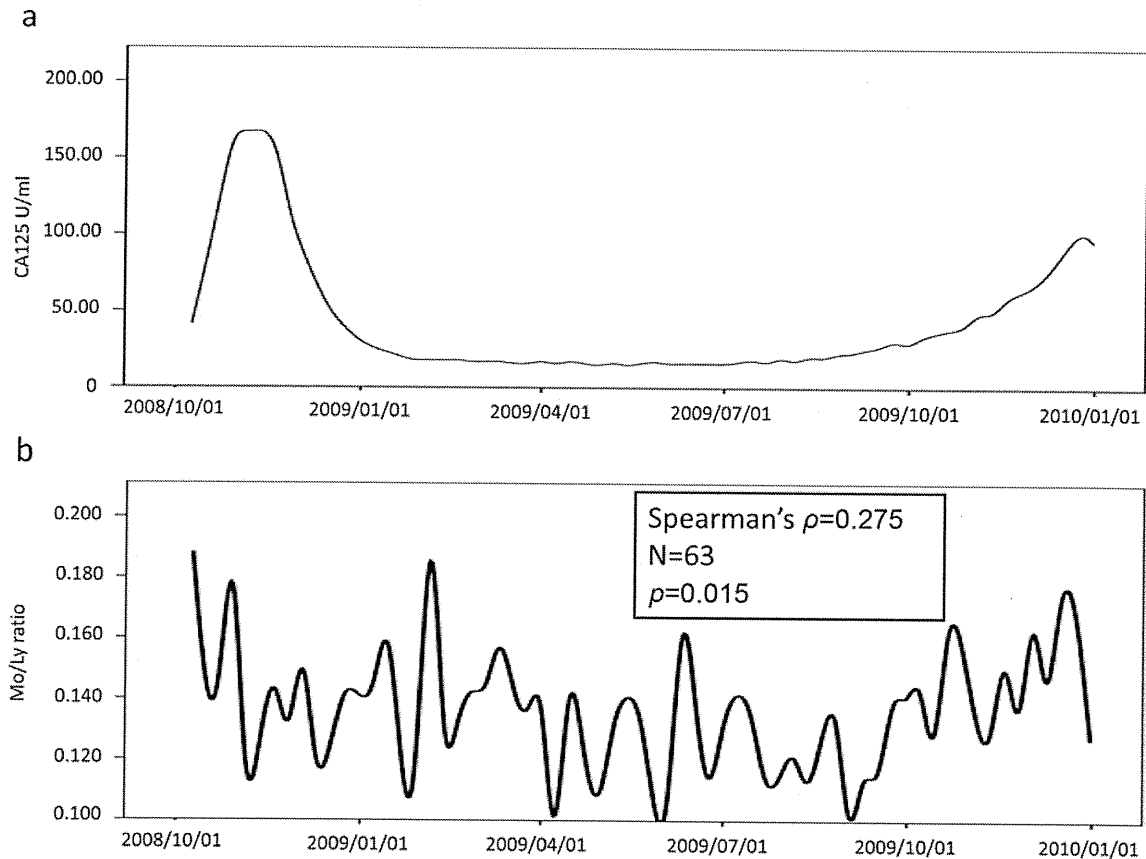


Figure 3. a: Time series of CA125 by WT1 peptide (weekly subcutaneous 3 mg injection). Normal level <35 units/ml. b: Time series of mononuclear phagocyte/lymphocyte ratios (Mo/Ly ratio). There was a weak positive correlation between CA125 and Mo/Ly ratio.

CA125 were observed. Despite the initial resistance to chemotherapy, stabilization of her disease for nearly a year suggests the efficacy of WT1 peptide vaccination.

Alterations of peripheral monocytes and lymphocytes might be good parameters for evaluating immunologic status and predicting recurrence in patients with gastric cancer (14). In our case, there was a weak positive correlation between CA125 and the Mo/Ly ratio (Spearman's $\rho=0.275$, $p=0.015$). We believe in this case that the Mo/Ly ratio indicated immunologic status and predicted recurrence.

Belli *et al.* reported that in a study of 28 patients with resected metastatic melanoma, two showed complete response and three manifested long-term disease stabilization with HSPPC-96 (autologous tumor-derived heat-shock protein GP96-peptide complex) vaccine (15). Bolonaki *et al.* also reported that disease stabilization occurred in 8 out of 22 patients with advanced non-small cell lung cancer vaccinated with an optimized cryptic human telomerase

reverse transcriptase peptide (16). Ohta *et al.* reported a case of WT1 peptide immunotherapy for metastatic childhood rhabdomyosarcoma, with patient remission continuing more than 22 months (17). This latter case is significant, as there are few reports of long-term WT1 peptide vaccination for cancer – apart from our own, where the vaccine stabilized intractable ovarian cancer over a year.

Unfortunately, the pathogenesis of ovarian cancer relapse is unknown. In addition, the immunotherapeutic mechanism of WT1 peptide and immunological escape mechanism for carcinoma cells remain to be elucidated.

Acknowledgements

This work was supported by a Grant-in-Aid for Young Scientists (B) and (A) (No. 19791140 and No. 21689044, respectively) from the Ministry of Education, Culture, Sports, Science and Technology, of the Japanese Government. We would like to thank J. Ishizaki, T. Umeda, H. Nakajima, T. Hakamata and C. Yoshikawa for their technical assistance and coordination of the clinical research.

References

- 1 Call KM, Glaser T, Ito CY, Buckler AJ, Pelletier J, Haber DA, Rose EA, Kral A, Yeger H, Lewis WH, Jones C and Housman DE: Isolation and characterization of a zinc finger polypeptide gene at the human chromosome 11 Wilms' tumor locus. *Cell* 60: 509-520, 1990.
- 2 Gessler M, Poustka A, Cavenee W, Neve RL, Orkin SH and Bruns GA: Homozygous deletion in Wilms tumors of a zinc-finger gene identified by chromosome jumping. *Nature* 343: 774-778, 1990.
- 3 Rivera MN and Haber DA: Wilms' tumour: connecting tumorigenesis and organ development in the kidney. *Nat Rev Cancer* 5: 699-712, 2005.
- 4 Sugiyama H: Wilms' tumor gene *WT1*: its oncogenic function and clinical application. *Int J Hematol* 73: 177-187, 2001.
- 5 Oka Y, Tsuboi A, Kawakami M, Elisseeva OA, Nakajima H, Udaka K, Kawase I, Oji Y and Sugiyama H: Development of WT1 peptide cancer vaccine against hematopoietic malignancies and solid cancers. *Curr Med Chem* 13: 2345-2352, 2006.
- 6 Yang L, Han Y, Suarez Saiz F and Minden MD: A tumor suppressor and oncogene: the *WT1* story. *Leukemia* 21: 868-876, 2007.
- 7 Nakatsuka S, Oji Y, Horiuchi T, Kanda T, Kitagawa M, Takeuchi T, Kawano K, Kuwae Y, Yamauchi A, Okamura M, Kitamura Y, Oka Y, Kawase I, Sugiyama H and Aozasa K: Immunohistochemical detection of WT1 protein in a variety of cancer cells. *Mod Pathol* 19: 804-814, 2006.
- 8 Ohno S, Dohi S, Ohno Y, Kyo S, Sugiyama H, Suzuki N and Inoue M: Immunohistochemical detection of WT1 protein in endometrial cancer. *Anticancer Res* 29: 1691-1695, 2009.
- 9 Oka Y, Tsuboi A, Murakami M, Hirai M, Tominaga N, Nakajima H, Elisseeva OA, Masuda T, Nakano A, Kawakami M, Oji Y, Ikegame K, Hosen N, Udaka K, Yasukawa M, Ogawa H, Kawase I and Sugiyama H: Wilms' tumor gene peptide-based immunotherapy for patients with overt leukemia from myelodysplastic syndrome (MDS) or MDS with myelofibrosis. *Int J Hematol* 78: 56-61, 2003.
- 10 Tsuboi A, Oka Y, Osaki T, Kumagai T, Tachibana I, Hayashi S, Murakami M, Nakajima H, Elisseeva OA, Fei W, Masuda T, Yasukawa M, Oji Y, Kawakami M, Hosen N, Ikegame K, Yoshihara S, Udaka K, Nakatsuka S, Aozasa K, Kawase I and Sugiyama H: WT1 peptide-based immunotherapy for patients with lung cancer: Report of two cases. *Microbial Immunol* 48: 175-184, 2004.
- 11 Oka Y, Tsuboi A, Taguchi T, Osaki T, Kyo T, Nakajima H, Elisseeva OA, Oji Y, Kawakami M, Ikegame K, Hosen N, Yoshihara S, Wu F, Fujiki F, Murakami M, Masuda T, Nishida S, Shirakata T, Nakatsuka S, Sasaki A, Udaka K, Dohy H, Aozasa K, Noguchi S, Kawase I and Sugiyama H: Induction of *WT1* (Wilms' tumor gene)-specific cytotoxic T lymphocytes by WT1 peptide vaccine and the resultant cancer regression. *Proc Natl Acad Sci USA* 101: 13885-13890, 2004.
- 12 Izumoto S, Tsuboi A, Oka Y, Suzuki T, Hashiba T, Kagawa N, Hashimoto N, Maruno M, Elisseeva OA, Shirakata T, Kawakami M, Oji Y, Nishida S, Ohno S, Kawase I, Hatazawa J, Nakatsuka S, Aozasa K, Morita S, Sakamoto J, Sugiyama H and Yoshimine T: Phase II clinical trial of Wilms' tumor 1 peptide vaccination for patients with recurrent glioblastoma multiforme. *J Neurosurg* 108: 963-971, 2008.
- 13 Ohno S, Kyo S, Myojo S, Dohi S, Ishizaki J, Miyamoto K, Morita S, Sakamoto J, Enomoto T, Kimura T, Oka Y, Tsuboi A, Sugiyama H and Inoue M: Wilms' tumor 1 (WT1) peptide immunotherapy for gynecological malignancy. *Anticancer Res* 29: 4779-4784, 2009.
- 14 Maeda H, Matsuzaki K, Miura O, Kawano T, Toda T, Minamisono Y, Nagasaki S and Ogoshi S: Quantitative alterations of peripheral monocytes and lymphocytes in patients with gastric cancer. *Jpn J Cancer Clin* 44(8): 799-803, 1998.
- 15 Belli F, Testori A, Rivoltini L, Maio M, Andreola G, Sertoli MR, Gallino G, Piris A, Cattelan A, Lazzari I, Carrabba M, Scita G, Santantonio C, Pilla L, Tragni G, Lombardo C, Arienti F, Marchiano A, Queriolo P, Bertolini F, Cova A, Lamaj E, Ascani L, Camerini R, Corsi M, Cascinelli N, Lewis JJ, Srivastava P and Parmiani G: Vaccination of metastatic melanoma patients with autologous tumor-derived heat-shock protein GP96-peptide complexes: clinical and immunologic findings. *J Clin Oncol* 20(20): 4169-4180, 2002.
- 16 Bolonaki I, Kotsakis A, Papadimitraki E, Aggouraki D, Konsolakis G, Vagia A, Christophylakis C, Nikoloudi I, Magganis E, Galanis A, Cordopatis P, Kosmatopoulos K, Georgoulis V and Mavroudis D: Vaccination of patients with advanced non-small cell lung cancer with an optimized cryptic human telomerase reverse transcriptase peptide. *J Clin Oncol* 25(19): 2727-2734, 2007.
- 17 Ohta H, Yoneda A, Takizawa S, Fukuzawa M, Tsuboi A, Murao A, Oji Y, Aozasa K, Nakatsuka S, Sugiyama H and Ozono K: WT1 (Wilms' tumor 1) peptide immunotherapy for childhood rhabdomyosarcoma: a case report. *Pediatr Hematol Oncol* 26: 74-83, 2009.

Received April 7, 2011

Revised May 26, 2011

Accepted May 27, 2011

Vaccination with WT-1 (Wilms' Tumor gene-1) peptide and BCG-CWS in melanoma

The Wilms tumor gene, WT1, plays an important role in the regulation of cell proliferation, differentiation, etc. Wild-type WT1 is highly expressed in malignancies, including malignant melanoma, and seems to be important for maintaining the transformed phenotype and function of cancer cells [1, 2]. The Bacillus Calmette-Guerin cell wall skeleton (BCG-CWS) activates dendritic cells via toll like receptors and is expected to be a useful adjuvant for cancer immunotherapy [3, 4]. We present a metastatic malignant melanoma patient who received clinical benefits and showed immunological response in association with using WT1 peptide vaccination with BCG-CWS.

A 64-year-old male with Stage IV malignant melanoma originating from the left chorioid, which had metastasized to the lungs, was admitted to Osaka University Hospital for WT1 peptide-based immunotherapy in February, 2008. In 2007, a lung nodule was histopathologically diagnosed as metastasis of malignant melanoma. The remaining metastatic lesion increased in size in spite of administration of the standard chemotherapy. The patient met the inclusion criteria for the vaccine trials, including having the HLA-A*2402 genotype and WT1 protein expression, and so was enrolled in the phase I clinical trial of immunotherapy using the WT1 peptide and BCG-CWS. According to the trial protocol, we used a modified 9-mer WT1 peptide, CYTWNQMNL. The treatment schedule was as follows; on day 1, 100 µg BCG-CWS was intracutaneously injected in the upper arm, followed by an injection of WT1 peptide (0.25 mg intracutaneously/0.25 mg subcutaneously) at the same site on day 2. The administrations were performed in the 1st, 3rd, 6th weeks and sequentially every month thereafter. With regard to adverse events, only a grade 2 skin ulcer was observed, which occurred at the injection site a few days after the injection, and lasted less than 2 months. Although the size of the target lesion measured by computed tomography had been steadily increasing before treatment, stable disease (SD) was achieved according to the Response Evaluation Criteria in Solid Tumors guidelines (figure 1A). Because no new metastatic lesions appeared for about 6 months after the beginning of vaccination, surgical resection of the right lower lobe, including the target lesion, was performed on day 188. Fluorescent immunostaining of the resected lung lesions before and after vaccination was performed.

The number of CD8⁺ T cells was robustly increased after vaccination (figures 1B-C). The delayed type hypersensitivity (DTH) reaction specific to the WT1 peptide shown by *in vivo* immuno-monitoring changed from negative to positive at one month after the first vaccination. For *ex vivo* immuno-monitoring, the frequencies

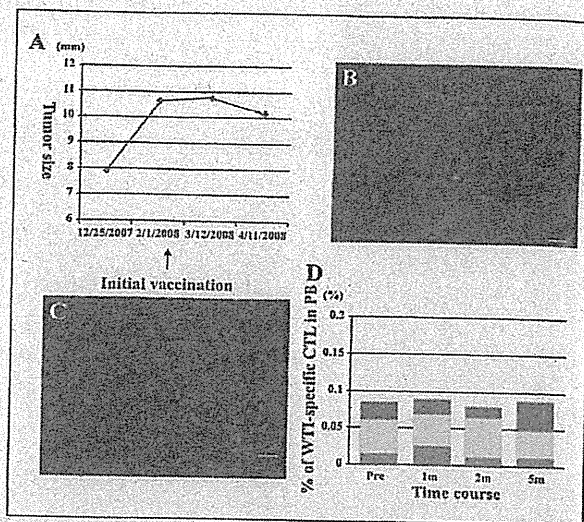


Figure 1. A) A graphical representation of the change in size of the target lesion in the lung. The tumor size was calculated by using computed tomography images, and the treatment response was evaluated according to the RECIST guidelines. The fluorescent immunostaining of the lung metastatic lesions before and after WT1 peptide vaccination. There were obviously more CD8⁺ T cells (red) after the vaccination (C) than before the vaccination (B). D) The frequencies of WT1-specific CTLs in peripheral blood and their subset compositions are shown. Based on CD45RA and CCR7 expression, the CTLs were phenotypically classified into four subsets; naïve (blue), central-memory (green), effector-memory (yellow), and effector (red).

of WT1-specific CTLs, determined by the percentages of WT1-tetramer⁺CD8⁺T cells among the total CD8⁺T cells in the peripheral blood, were measured (figure 1D). Furthermore, based on CD45RA and CCR7 expressions, a phenotype analysis of the CTLs was performed, in which they were classified into naïve (blue), central-memory (green), effector-memory (yellow), and effector (red) subsets. The frequency of WT1-specific CTLs remained at about 0.07% before and after vaccination. WT1-specific CTLs in effector-memory and effector subsets accounted for the dominant CTL populations both before and after the vaccination. The frequency of WT1-specific CTLs was not higher than that in healthy donors, in whom WT1-specific CTLs in the naïve subset were dominant [5]. Such a high percentage of well-differentiated WT1-specific CTLs even before treatment might have contributed to the induction of a clinical response. Taken together, these findings suggest that WT1 peptide vaccination with a BCG-CWS adjuvant induced a stabilization of the disease, associated with induction of a WT1 peptide-specific immune-response and infiltration of CD8⁺ T cells in the tumor tissue, offering evidence for the therapeutic potential of this treatment for malignant melanoma. ■

Disclosure. Acknowledgement: We thank Ms. Kana Hasegawa, Kazuko Takahashi and Tomoe Umeda for their excellent technical support and Masayoshi Inoue for surgical resection of the lung metastatic lesion. Financial

support: This work was supported in part by a grant from the Ministry of Education, Culture, Sports, Science and Technology of Japan and a grant from the Ministry of Health, Labor and Welfare. Conflict of Interest: none.

¹ Department of Dermatology,

² Department of functional Diagnostic Science,

³ Department of Cancer Immunotherapy,

⁴ Department of Cancer Stem Cell Biology

⁵ Department of Respiratory Medicine, Allergy and Rheumatic Diseases,

Osaka University Graduate School of Medicine,

2-2, Yamadaoka Suita-shi,

Osaka 565-0871,

Japan

⁶ Professor Emeritus of Hokkaido University,

Japan

^a These authors contributed equally to

this work.

<tanemura@derma.med.osaka-

u.ac.jp>

1. Nakatsuka S, Oji Y, Horiuchi T, et al. Immunohistochemical detection of WT1 protein in a variety of cancer cells. *Mod Pathol* 2006; 19:804-814.

2. Oka Y, Tsuboi A, Fujiki F, et al. "Cancer antigen WT1 protein-derived peptide"-based treatment of cancer toward the further development. *Curr Med Chem* 2008; 15:3052-3061.

3. Tsuji S, Matsumoto M, Takeuchi O, et al. Maturation of human dendritic cells by cell wall skeleton of *Mycobacterium bovis* bacillus Calmette-Guérin: involvement of toll-like receptors. *Infect Immun* 2000; 68:6883-6890.

4. Nakajima H, Kawasaki K, Oka Y, et al. WT1 peptide vaccination combined with BCG-CWS is more efficient for tumor eradication than WT1 peptide vaccination alone. *Cancer Immunol Immunother* 2004; 53:617-624.

5. Kawakami M, Oka Y, Tsuboi A, et al. Clinical and immunologic responses to very low-dose vaccination with WT1 peptide (5 microg/body) in a patient with chronic myelomonocytic leukemia. *Int J Hematol* 2007; 85:426-429.

Megumi NISHIOKA^{1,a}

Atsushi TANEMURA^{1,a}

Sumiyuki NISHIDA^{3,a}

Akiko NAKANO²

Akihiro TSUBOI³

Yusuke OJI⁴

Yoshihiro OKA⁵

Ichiro AZUMA⁶

Haruo SUGIYAMA²

Ichiro KATAYAMA¹

the central and left face. The tumour was densely infiltrated with multilocular ulcerations and brownish crusts, leading to a facies leonina-like appearance (figure 1A). There were no B-symptoms like fatigue, night sweats or weight loss. Despite previous histological investigations, the underlying cause of disease was still unclear. Under the suspected diagnosis of pyoderma, an antibiotic and steroid based therapy was initiated (sultamicillin 375 mg BID; erythromycin 500 mg BID; minocyclin 100 mg OD; prednicarbate locally BID). However, no response to therapy was observed, and the patient was transferred to our department.

Except for local symptoms on the face, physical examinations showed no other abnormal findings. Two new skin biopsies were taken. Histopathology revealed dense inflammatory infiltrates predominantly in the middle part of the dermis, clustering around destructed hair follicles (figure 1C). Higher magnification unveiled a polymorphic folliculotropic lymphoid infiltrate with atypical features, containing limited numbers of eosinophils and plasma cells (figure 1D). Alcian-PAS staining demonstrated deposits of mucin, especially in the areas of hair follicles. By immunohistochemical examination, lymphocytes stained positively for CD3, CD4 and CD45 RO. Approximately 10% of lymphoid cells were positive for the proliferation marker Mib-1. Multiplex-PCR verified clonality of the T cell receptor gamma chain.

Based on clinical appearance, histopathology and molecular findings, folliculotropic mycosis fungoides was diagnosed. Using imaging techniques (CT scans, ultrasound) and peripheral blood smear stainings, an extracutaneous involvement was ruled out. We initiated a combined therapy with oral psoralen (40 mg meladinine prior to irradiation)



Figure 1. A) At presentation, densely infiltrated plaques with crusts and ulcerations were present on the central and left face, giving the patient a facies leonina-like appearance. B) 10 months after initiation of combined therapy with oral bexarotene and PUVA, lesions had cleared almost completely. C) Histopathology of skin biopsies showed dense inflammatory infiltrates in the dermis, especially around destructed hair follicles (H&E, $\times 50$). D) Higher magnification ($\times 200$) reveals infiltration of hair follicles by lymphoid cells with atypical features.

Successful treatment of a folliculotropic mycosis fungoides with bexarotene and PUVA

According to the WHO-EORTC classification of primary cutaneous lymphomas, follicular mycosis fungoides (FMF) is a rare subtype of mycosis fungoides, the most common form of cutaneous T cell lymphoma. In comparison to classical MF, FMF often shows a more aggressive clinical course, with 5 year survival rates of only 64% [1]. We report a 69-year-old woman who presented with a 3-year history of a slowly-growing, well-demarcated, red tumor in

CD166/Activated leukocyte cell adhesion molecule is expressed on glioblastoma progenitor cells and involved in the regulation of tumor cell invasion

Noriyuki Kijima, Naoki Hosen, Naoki Kagawa, Naoya Hashimoto, Akiko Nakano, Yasunori Fujimoto, Manabu Kinoshita, Haruo Sugiyama, and Toshiki Yoshimine

Department of Neurosurgery, Osaka University Graduate School of Medicine, Osaka, Japan (N.K., N.K., N.H., Y.F., M.K., T.Y.); Department of Functional Diagnosis, Osaka University Graduate School of Medicine, Osaka, Japan (N.H., H.S.); Department of Medicine, University of Montreal, CHM-Hospital Notre-Dame and CHM Research Center, Montreal, Quebec, Canada (A.N.)

For improvement of prognosis for glioblastoma patients, which remains poor, identification and targeting of glioblastoma progenitor cells are crucial. In this study, we found that the Cluster of Differentiation (CD)166/activated leukocyte cell adhesion molecule (ALCAM) was highly expressed on CD133⁺ glioblastoma progenitor cells. ALCAM⁺CD133⁺ cells were highly enriched with tumor sphere-initiating cells *in vitro*. Among gliomas with isocitrate dehydrogenase-1/R132H mutation, the frequencies of ALCAM⁺ cells were significantly higher for glioblastomas than for World Health Organization grade II or III gliomas. The function of ALCAM in glioblastoma was then investigated. An *in vitro* invasion assay showed that transfection of ALCAM small interfering RNA or small hairpin RNA into glioblastoma cells significantly increased cell invasion without affecting cell proliferation. A soluble isoform of ALCAM (sALCAM) was also expressed in all glioblastoma samples and at levels that correlated well with ALCAM expression levels. *In vitro* invasion of glioblastoma cells was significantly enhanced by administration of purified sALCAM. Furthermore, overexpression of sALCAM in U87MG glioblastoma cells promoted tumor progression *in i.c.* transplants into immune-deficient mice. In summary, we were able to show that ALCAM constitutes a novel glioblastoma progenitor cell marker. We could also demonstrate that

ALCAM and its soluble isoform are involved in the regulation of glioblastoma invasion and progression.

Keywords: activated leukocyte cell adhesion molecule, cancer stem cell, CD166, glioblastoma, invasion.

Glioblastoma is one of the most frequently occurring malignancies in the CNS. Despite intensive treatment, including surgery, radiation, and chemotherapy, the prognosis for glioblastoma is still very poor, and the median survival time is only 12–15 months.¹ One major reason for the extremely poor prognosis is that glioblastoma progenitor cells possessing tumor-initiating ability^{2,3} are resistant to radiation and chemotherapy.⁴ Glioblastoma progenitor cells reportedly exist in the Cluster of Differentiation (CD)133⁺ glioblastoma cell population.² While CD133 is the most promising marker for the identification of glioblastoma progenitor cells, additional cell surface markers for glioblastoma progenitor cells are needed for more efficient enrichment of these cells and identification of their location in a microenvironment. Recently, stage-specific embryonic antigen-1,⁵ A2B5,⁶ neural cell adhesion molecule L1,⁷ and integrin alpha-6⁸ have been mentioned as candidates for novel glioblastoma stem/progenitor cell markers.

One main source of the high malignancy of glioblastoma is the invasion of isolated tumor cells into the surrounding parenchyma.⁹ It is therefore important to clarify the molecular mechanism of this strong invasiveness of glioblastoma cells, and several molecules, such as cadherin,¹⁰ neural cell adhesion molecule,¹¹ and integrin,¹² are reportedly involved in glioblastoma invasion.

Received June 6, 2011; accepted October 26, 2011.

Corresponding Author: Naoki Hosen, Department of Functional Diagnosis, Osaka University Graduate School of Medicine, 1-7 Yamadaoka, Suita, Osaka, 565-0871, Japan (hnaoki@imed3.med.osaka-u.ac.jp).

The CD166/activated leukocyte cell adhesion molecule (ALCAM) is a member of the immunoglobulin superfamily and is widely expressed in various tissues, such as neurons, fibroblasts, endothelial cells, and keratinocytes.^{13–15} ALCAM is involved in neurogenesis,¹³ angiogenesis, hematopoiesis,¹⁶ leukocyte trafficking,¹⁷ and hematopoietic stem cell maintenance in bone marrow niches.¹⁸ It is reported to be a cell surface marker for mesenchymal stem cells^{19,20} and hematopoietic progenitor cells.^{16,21} It is also expressed in several kinds of cancer and is reportedly a marker for cancer stem cells in colon cancer²² and prostate cancer.²³ However, there have been no reports about ALCAM expression on glioblastoma cells. On the other hand, functional roles of ALCAM have been investigated in several kinds of cancer,²⁴ especially in metastatic melanoma, in which it functions as a cell surface sensor for cell density and controls the transition from local cell proliferation to tissue invasion.^{25,26} Moreover, ALCAM was found to be required for promoting cell invasion because of its efficient triggering of the activation of the metalloproteinase cascade in response to extensive cell-to-cell and cell-to-matrix contacts.²⁵

The soluble isoform of ALCAM (sALCAM) was isolated as an alternative short ALCAM transcript comprising only the first 3 exons.²⁷ Since the sALCAM protein possesses the immunoglobulin domain D1, which is required for homophilic ALCAM binding, sALCAM impairs cell-to-cell interaction through homophilic ALCAM binding,²⁷ and as a result affects the coordination of local tumor growth, invasion, and metastasis.²⁸ It was also reported that sALCAM attenuates melanoma invasion.²⁸

In this study, we examined whether ALCAM could serve as a progenitor cell marker for glioblastoma, while the clinical significance of ALCAM as an indicator of the histological grade or as a prognostic factor was also investigated. In addition, we investigated the functional roles of ALCAM and sALCAM in glioblastoma.

Materials and Methods

Glioma Samples and Clinical Data

For fluorescence activated cell sorter (FACS) analysis, 12 glioblastoma samples from patients who had undergone surgery at Osaka University Hospital between 2007 and 2008 were analyzed. For immunohistochemical analysis, formalin-fixed paraffin-embedded (FFPE) glioma samples from patients who had undergone surgery at Osaka University Hospital between 2003 and 2010 were analyzed. For Kaplan–Meier analysis, we obtained clinical data to estimate progression-free survival (PFS) and overall survival (OS) from our database or medical records of glioblastoma patients who had undergone maximal surgical resection and chemoradiation therapy between 2005 and 2010 at Osaka University Hospital.

This study was approved by the institutional review board of Osaka University School of Medicine. The

details of the study were explained to glioma patients before they underwent surgery at Osaka University Hospital. When written agreement had been obtained from a patient for the use of the resected tissue for this research, a part of the tissue was subjected to the analyses in this study.

FACS Analysis

Glioblastoma samples were first minced with a scalpel and then dissociated using a neural cell dissociation kit containing papain (Miltenyi Biotec), according to the manufacturer's instructions. Single-cell suspensions generated from the glioblastoma samples were stained with biotin-conjugated anti-CD133 monoclonal antibody (mAb) (AC133; Miltenyi Biotec), phycoerythrin-conjugated anti-ALCAM mAb (3A6; BD Pharmingen), CD45-allophycocyanin (APC) (BD Pharmingen), CD31-APC (eBioscience), and then with streptavidin-fluorescein isothiocyanate (BD Pharmingen) or Cy7PE (eBioscience). The stained suspensions were then analyzed on FACS Aria flow cytometer (Becton Dickinson).

Tumor-Sphere Formation Assay

Five hundred FACS-sorted cells were seeded in 96-well plates and cultured in a serum-free medium supplemented with 20 ng/mL of epidermal growth factor (R&D Systems), 20 ng/mL of basic fibroblast growth factor (Peprotech), and 20 ng/mL of leukemia inhibitory factor (Millipore) in 5% CO₂. Cells were nourished every 2 days by refreshing half of the medium. The tumor spheres were counted 14 days after the seeding.

Quantitative PCR

Total RNA was extracted from the glioma cell line and primary glioblastoma samples using Trizol (Invitrogen Life Technologies) according to the manufacturer's instructions. cDNA was generated using Moloney murine leukemia virus reverse transcriptase (Promega) and then subjected to quantitative PCR with SYBR (Synergy Brands) green in an Applied Biosystems 7900HT system. To measure ALCAM or sALCAM expression, the following primers were used: for ALCAM: CGTGAATTCCACCAAGAAGGAGGAGGA for sense primers and TCTGTCITTTGTATTCTGGT ACATCG for antisense primers; for sALCAM: AGAC AGATTGAACCTCTCTCAGAAAAC for sense primers and GCTGCAGACTACTTACTGAACACC for antisense primers.

Knockdown of ALCAM Expression by siRNA and shRNA

Anti-ALCAM small interfering (si)RNA, short hairpin (sh)RNA, or control RNA was transfected to U87MG and U251 cells (American Type Culture Collection) using Lipofectamine RNAiMAX reagent (Invitrogen). Sequences of siRNAs specific for ALCAM were:

siRNA1: UCUACAAUGAGAGUCAUUGACUCUC and GAGAGUCAUUGACUCUCAUUGUAGA, siRNA2: A GUAAUUGUCCACUGAAUGGCUGGC and GCCAG CCAUUCAGUGGACAAUUACU. Stealth RNA interference negative control (Invitrogen) was used as the negative control siRNA. Two days after transfection, cells were subjected to FACS analysis for detection of ALCAM expression and to a Matrigel invasion assay. The cell proliferation assay was started soon after siRNA transduction.

To establish cell lines in which ALCAM expression was stably knocked down, we used a Mission shRNA (Sigma Aldrich) lentivirus carrying an shRNA sequence against ALCAM (CCGGCAGCCATGATAATAGGT CATACTCGAGTATGACCTATTATCATGGCTGTTT TTG). Lentivirus was produced by transfection of the lentiviral vector with the gag-pol-expressing vector and the vector expressing a vesicular stomatitis virus-glycoprotein envelope (both were kindly donated by Hiroyuki Miyoshi). Viruses were concentrated by centrifugation with PEG-it (System Bioscience). U87MG and U251 glioblastoma cells were infected with lentivirus carrying ALCAM-shRNA. Knockdown of ALCAM was confirmed by FACS analysis.

Generation of sALCAM Isoform-Expressing Glioblastoma Cells

The expression vector carrying flag-tagged sALCAM cDNA (sALCAM-p3XFLAG) (Sigma Aldrich)²⁷ was kindly donated by Koji Ikeda MD of Kyoto Prefectural University of Medicine. U87MG glioblastoma cells were transduced with flag-tagged sALCAM cDNA by means of electroporation. Stable transfectants were selected by culturing cells in medium supplemented with 500 µg/mL of G418 (Roche). The sALCAM-Flag protein was detected by western blotting using anti-Flag M2 antibody (Sigma Aldrich) and anti-mouse immunoglobulin G-alkaline phosphatase (Santa Cruz Biotechnology). The sALCAM-Flag protein was purified from U87MG expressing sALCAM-Flag cells using anti-Flag affinity gel (Sigma Aldrich) according to the manufacturer's instructions.

Invasion Assay

The invasiveness of U87MG and U251 cells was assayed with a modified Boyden Chamber Matrigel method²⁹ using the Biocoat Matrigel invasion chamber (Becton Dickinson Bioscience) according to the manufacturer's instructions. Cells were washed with phosphate buffered saline (PBS) and harvested using a cell dissociation buffer (Invitrogen), after which 2.5×10^4 cells in serum-free Dulbecco's modified Eagle's medium (DMEM) were seeded onto Matrigel-coated filters. DMEM containing 10% fetal bovine serum was added to the lower compartment, and cells were incubated for 48 h. After removal of the cells that remained in the top chamber, the top surface of each membrane was cleared of cells with a cotton swab. Cells that had penetrated to the

bottom side of the membrane were then fixed in buffered formalin, stained with a Diff-Quik Stain Set (Wako), and counted.

Gelatin Zymography

The same number of cells (5×10^5) were placed in 100 µL of serum-free medium (DMEM/F12 Ham's) and incubated for 24 h. Supernatant from each well was subjected to gelatin zymography with zymogram gel (Tris-glycine; Invitrogen) according to the manufacturer's instructions. The gels were then stained with Coomassie brilliant blue R-250.

Intracranial Xenograft Model

Newborn Rag2^{-/-}γc^{-/-} mice (kindly donated by Irving Weissman, MD, of Stanford University) were used as recipients. Pups were anesthetized on ice, and glioblastoma cells (2×10^5) in 2 µL of PBS were injected into the right lateral ventricle with a stereotactic injector (Stoelting).

Immunohistochemical Analysis

For double immunostaining, indirect immunoalkaline phosphatase and immunoperoxidase methods were used. Fresh frozen glioblastoma tissue sections (6 µm) were fixed in pure acetone for 10 min and then in a formol-calcium solution for 1 min after rehydration in PBS. After washing in PBS and incubation with a blocking solution (Block Ace; DS Pharma Biomedical) for 10 min, the sections were incubated with the first mAb, anti-CD166 (3A6; Abcam), for 1 h at room temperature. Each subsequent step was followed by washing 3 times with PBS for 2 min. Bound mAb was detected with an alkaline phosphatase-labeled second antibody for 20 min, and the sections were fixed further with 1% glutaraldehyde (Nacalai Tesque) in PBS for 30 s. The labeled cells were then colored red with Alkaline Phosphatase Substrate Kit I (Vector red; Vector Laboratories). The sections were then incubated with the biotin-labeled second mAb, anti-CD31 (eBioscience), reacted with streptavidin peroxidase (N-Histofine; Nichirei), and colored brown with 3,3'-diaminobenzidine (DAB) hydrochloride (Histofine Simple Stain DAB; Nichirei). Levamisole (Sigma Chemical) and hydrogen peroxide solution (Nacalai Tesque) were used to inhibit endogenous alkaline phosphatase and peroxidase activity, respectively. The sections were counterstained with Lillie-Mayer's hematoxylin solution (Wako) and mounted in Aquatex (Merck).

FFPE glioma samples were also stained with anti-ALCAM mAb (3A6; Abcam) and anti-IDH1-R132H mAb (H09; Dianova). The histofine simple stain MAX-PO (Multi; Nichirei) was used as a secondary antibody. For visualization, the specimens were reacted with 3,3'-DAB tetrahydrochloride (Dojindo).

Statistical Analysis

Student's *t*-test was used to determine statistical significance for the in vitro experiments. For the analysis of clinical data and in vivo experiments, Kaplan–Meier analysis and the Wilcoxon test were used. For all analyses, differences were defined as statistically significant at $P < .05$.

Results

ALCAM Is a Glioblastoma Progenitor Cell Marker

ALCAM expression on CD31⁻CD45⁻CD133⁺ glioblastoma cells (CD133⁺ glioblastoma cells) or CD31⁻CD45⁻CD133⁻ glioblastoma cells (CD133⁻ glioblastoma cells) was subjected to FACS analysis. Ratios of ALCAM⁺ cells were significantly ($P < .05$, $n = 12$) higher in the CD133⁺ glioblastoma cell population ($37.0 \pm 10.1\%$ [1.9%–95.4%]) than in the CD133⁻ cell population ($17.4 \pm 6.2\%$ [0%–57.6%]) (Fig. 1A). CD133⁺ glioblastoma cells could be separated into an ALCAM⁺ and an ALCAM⁻ population. To examine whether ALCAM⁺CD133⁺ glioblastoma cells were enriched with glioblastoma progenitor cells, a tumor-sphere formation assay was performed with fluorescence activated cell sorted ALCAM⁺CD133⁺ or ALCAM⁻CD133⁺ glioblastoma cells. Five glioblastoma samples were examined, and cells that formed tumor spheres accounted for 4.6 ± 0.4 per 500 cells in the ALCAM⁺CD133⁺ fraction, and for 0.6 ± 0.6 per 500 cells in the ALCAM⁻CD133⁺ fraction ($P < .05$, Fig. 1B). These results indicate that ALCAM in combination with CD133 can be used as a glioblastoma progenitor cell marker. Furthermore, in a glioblastoma sample that contained no CD133⁺ cells, only ALCAM⁺ cells formed tumor spheres (Fig. 1C), showing that ALCAM is a potential marker for glioblastoma progenitor cells even in CD133⁻ glioblastoma samples. Immunohistochemical analysis with anti-ALCAM mAb identified distinct ALCAM⁺CD31⁻ glioblastoma cells, whereas endothelial cells were ALCAM⁺CD31⁺ (Fig. 1D).

Frequency of ALCAM⁺ Cells Correlates with Histological Grade in IDH1-R132H Mutation-Positive Glioma and Prognosis for IDH1-R132H Mutation-Negative Primary Glioblastoma Patients

It is now known that World Health Organization (WHO) grade II gliomas are almost uniformly characterized by isocitrate dehydrogenase (IDH)-1 mutations, while most primary glioblastomas are IDH1 wild type.^{30–33} In addition, the presence of IDH1 mutation reportedly correlates well with positive staining for anti-IDH1-R132H mAb in immunohistochemical studies.^{34,35} IDH1-R132H⁺ glioma samples (Fig. 2A) were examined for ALCAM expression. For this analysis, we used 16 WHO grade II glioma samples (10 diffuse astrocytomas, 3 oligoastrocytomas, and 3

oligodendrogliomas), 10 WHO grade III glioma samples (6 anaplastic astrocytomas, 3 anaplastic oligoastrocytomas, and 1 anaplastic oligodendroglioma), and 9 glioblastoma samples. The percentages of ALCAM⁺ cells were 27.7 ± 9.1 , 29.4 ± 20.2 , and $48.7 \pm 8.9\%$ for WHO grades II, III, and IV, respectively (Fig. 2B). The frequency of ALCAM⁺ cells was significantly ($P < .05$) higher in glioblastomas than in WHO grade II or III gliomas.

We also examined whether the frequencies of ALCAM⁺ cells correlated with the prognosis for primary glioblastoma (IDH1-R132H mutation⁻) patients. PFS and OS were compared for glioblastoma patients with a high percentage and those with a low percentage of ALCAM⁺ cells. At a cutoff value of 60% ALCAM⁺ cells, median PFS for the patients with a high percentage of ALCAM⁺ cells (115.75 ± 67.41 days, $n = 12$) was significantly ($P < .05$) higher than for their low-percentage counterparts (447.97 ± 308.36 days, $n = 27$) (Fig. 2C). The corresponding median OS was 275.77 ± 151.27 and 731.61 ± 300.69 days ($P < .05$) (Fig. 2C). However, at a cutoff value of 50% or less of ALCAM⁺ cells, the difference in PFS or OS was not statistically significant (data not shown).

ALCAM Is Involved in the Regulation of Glioblastoma Cell Invasion

The functional roles of ALCAM in glioblastoma were investigated next. Two sequences of siRNA specific for ALCAM were used for knocking down ALCAM in glioblastoma cells. A comparison between cell growth of anti-ALCAM siRNA-transfected and negative control siRNA-transfected U87MG glioblastoma cells (Fig. 3A) showed that the reduction in ALCAM expression had no effect on cell growth (Fig. 3B). We then used a modified Boyden Chamber Matrigel assay to examine the effects of ALCAM knockdown on U87MG and U251 glioblastoma cell invasion. The numbers of cells that reached the bottom of the filters through the Matrigel were 23.3 ± 6.8 , 66.7 ± 12.9 , and 5.7 ± 1.9 of the ALCAM siRNA1, ALCAM siRNA2, and negative control siRNA-transfected U87MG cells, respectively, and were 221.2 ± 9.3 and 50.2 ± 8.4 of the ALCAM shRNA- and negative control-transfected U251 cells, respectively (Fig. 3C), indicating that downregulation of ALCAM expression of glioblastoma cells significantly ($P < .05$) enhanced tumor cell invasion. Conditioned media from cultures of ALCAM siRNA- or negative control siRNA-transfected U87MG cells were analyzed with gelatin zymography. Conversion of promatrix metalloproteinase (MMP)-2 to active MMP-2 was observed in both of the conditioned media, while there was no difference in the quantity of active MMP-2 between ALCAM siRNA-transfected U87MG and control siRNA-transfected cells (Fig. 3D).

The soluble isoform of ALCAM (sALCAM) expressed in glioblastoma cells enhances cell invasion in vitro and promotes tumor progression in vivo.

Endogenous expression levels of ALCAM and sALCAM in primary glioblastoma samples were examined

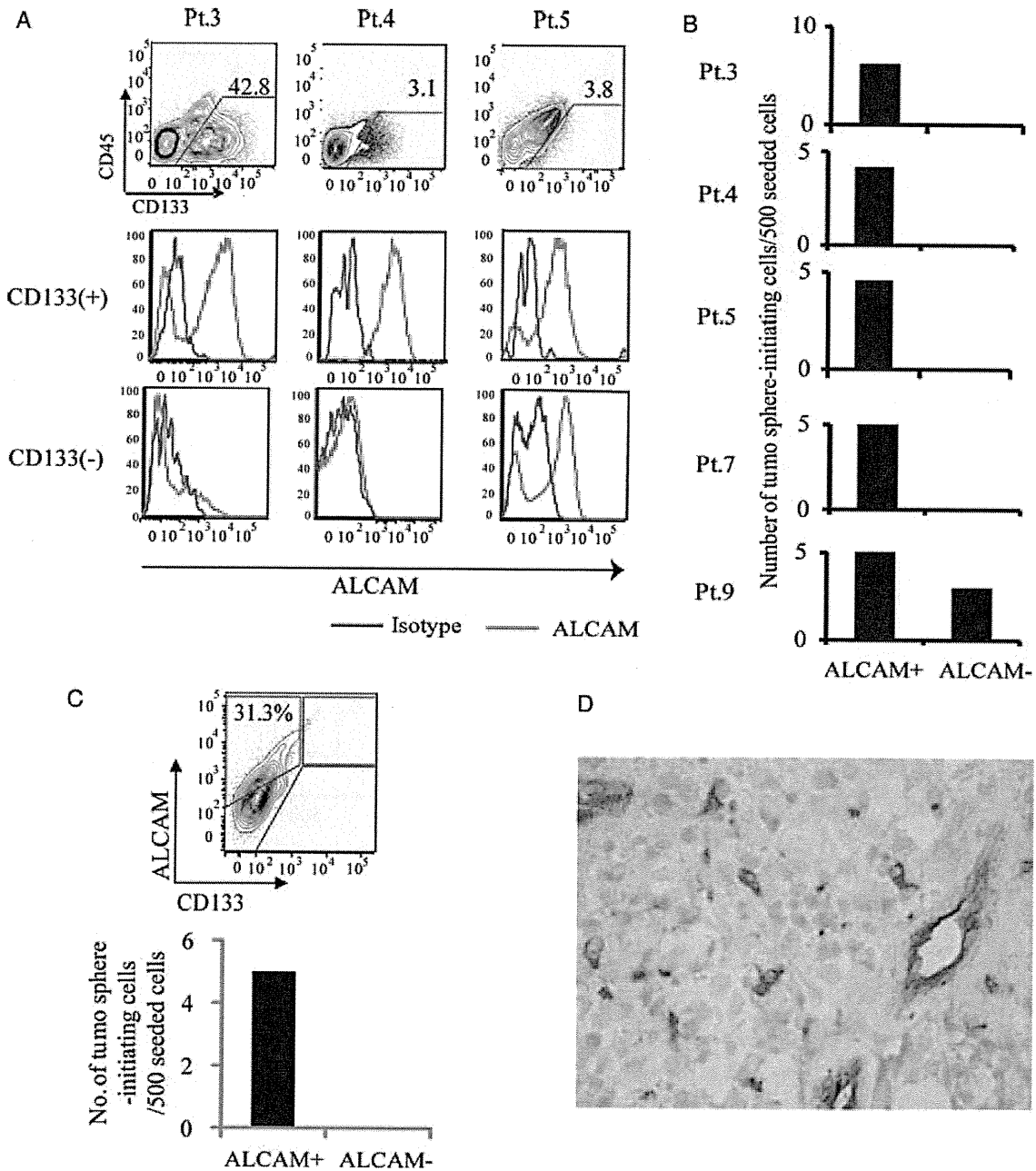


Fig. 1. ALCAM is a glioblastoma progenitor cell marker. (A) Flow cytometric analyses of CD45⁻CD31⁻ cells from glioblastoma samples. Three representative cases are shown. CD45⁻CD31⁻ cells were separated into CD133⁺ and CD133⁻ cell populations and then analyzed for ALCAM expression. (B) Tumor-sphere formation assays using FACS-sorted CD133⁺ALCAM⁺ cells or CD133⁺ALCAM⁻ glioblastoma cells. (C) Tumor-sphere assays using CD133⁻ALCAM⁺ cells or CD133⁻ALCAM⁻ cells in a glioblastoma sample that contained no CD133⁺ cells. (D) Immunohistochemical staining of ALCAM and CD31 expression on glioblastoma samples. Red (vector red): ALCAM; brown (DAB):CD31.

by using quantitative real-time PCR (Fig. 4A). All primary glioblastoma samples expressed sALCAM. In addition, sALCAM expression levels in glioblastoma samples correlated well with ALCAM expression levels (Fig. 4A).

To examine the functional role of sALCAM in glioblastoma cells, U87MG cells transduced with

sALCAM-Flag or an empty vector (U87MG-sALCAM or U87MG-mock) were generated (Fig. 4B). There was no difference in cell proliferation between U87MG-mock and U87MG-sALCAM cells (Fig. 4C). We next used a modified Boyden Chamber Matrigel assay to examine whether sALCAM was involved in

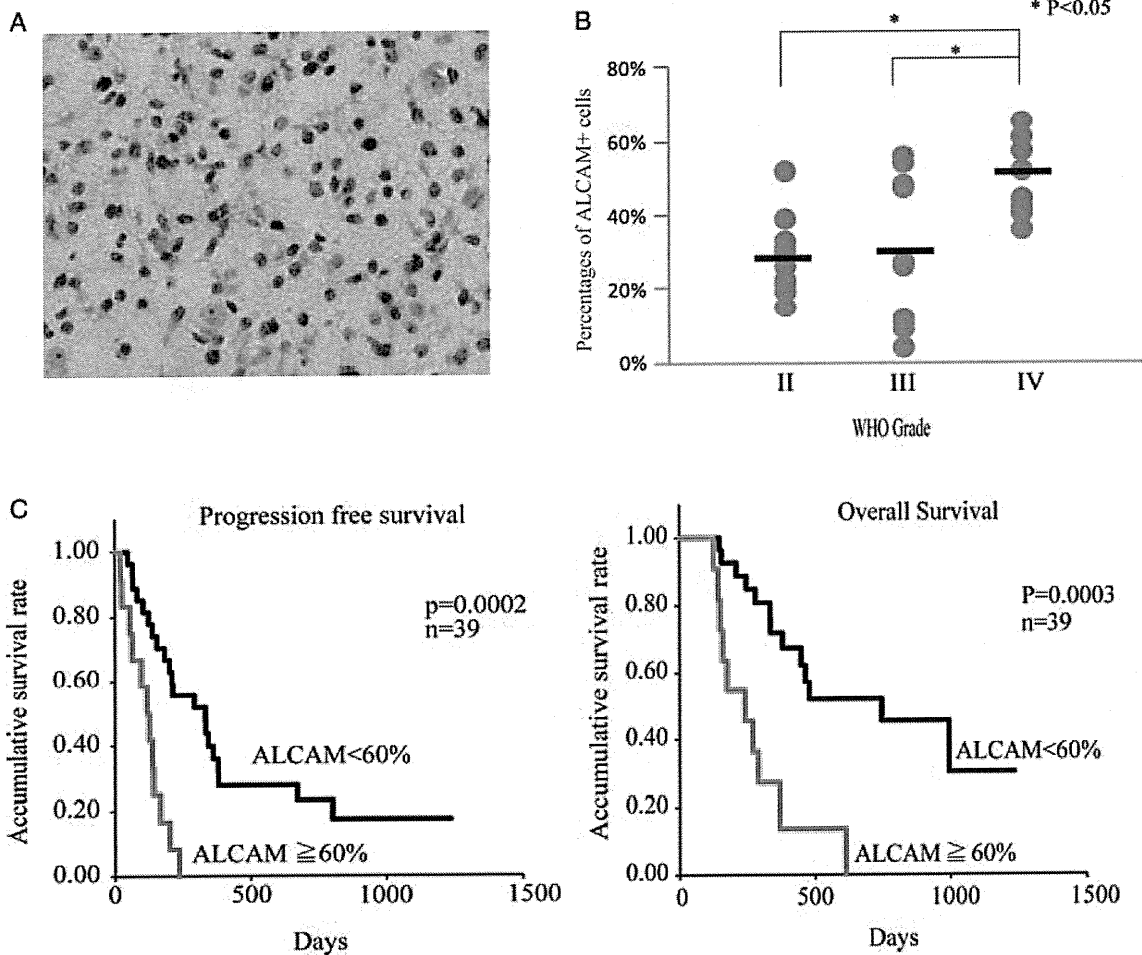


Fig. 2. ALCAM expression correlates with histological grade of glioma and prognosis for glioblastoma patients. (A) Immunohistochemical staining of anti-IDH1-R132H mAb in astrocytoma samples. (B) Percentages of ALCAM⁺ cells in IDH1-R132H mutation+ WHO grades II-IV glioma specimens. The horizontal bar shows the average percentages of ALCAM⁺ glioblastoma cells. (C) Plots for progression-free survival and overall survival of primary glioblastoma patients with high percentages (≥60%) and of those with low percentages (<60%) of ALCAM⁺ cells.

glioblastoma cell invasion. The numbers of cells that reached the bottom of the filters through the Matrigel were 30.8 ± 13.2 , 27.0 ± 4.8 , and 5.8 ± 1.8 of the U87MG-sALCAM clone 1, U87MG-sALCAM clone 2, and U87MG-mock cells, respectively. These results indicate that sALCAM expression in glioblastoma cells significantly ($P < .05$) enhances tumor cell invasion (Fig. 4D). Conditioned media from cultures of U87MG-sALCAM or U87MG-mock cells were also analyzed by means of gelatin zymography. Conversion of pro-MMP-2 to active MMP-2 was observed in both of the conditioned media, while there was no difference in the amount of active MMP-2 between ALCAM siRNA-transfected U87MG and control siRNA-transfected cells.

Western blotting with anti-Flag mAb led to the detection of sALCAM-Flag protein in the culture supernatant of U87MG-sALCAM cells (Fig. 4E). We used the anti-Flag affinity gel to purify the sALCAM-Flag

protein (Fig. 4E) and then examined with an in vitro invasion assay whether this purified sALCAM protein promoted the invasion of glioblastoma cells. We found that the ability of invasion of U87MG and U251 cells was significantly ($P < .05$) increased by the addition of purified sALCAM, with the effect depending on the quantity added (Fig. 4F). This result makes it clear that sALCAM promotes the invasion of glioblastoma cells.

Next, we examined the effect of sALCAM on glioblastoma progression in vivo. Two clones of U87MG-sALCAM or U87MG-mock cells were injected i.c. into the right ventricle of the newborn pups of Rag2^{-/-}γc^{-/-} mice. Two independent clones of the U87MG-sALCAM cells were examined. Difference in the survival curve was significant ($P < .05$) for mice injected with sALCAM-expressing U87MG cells (both clone 1 and clone 2) and those with U87MG-mock cells, but was not significant for sALCAM-expressing clones 1 and 2 (Fig. 5A). All of the mice ($n = 8$)

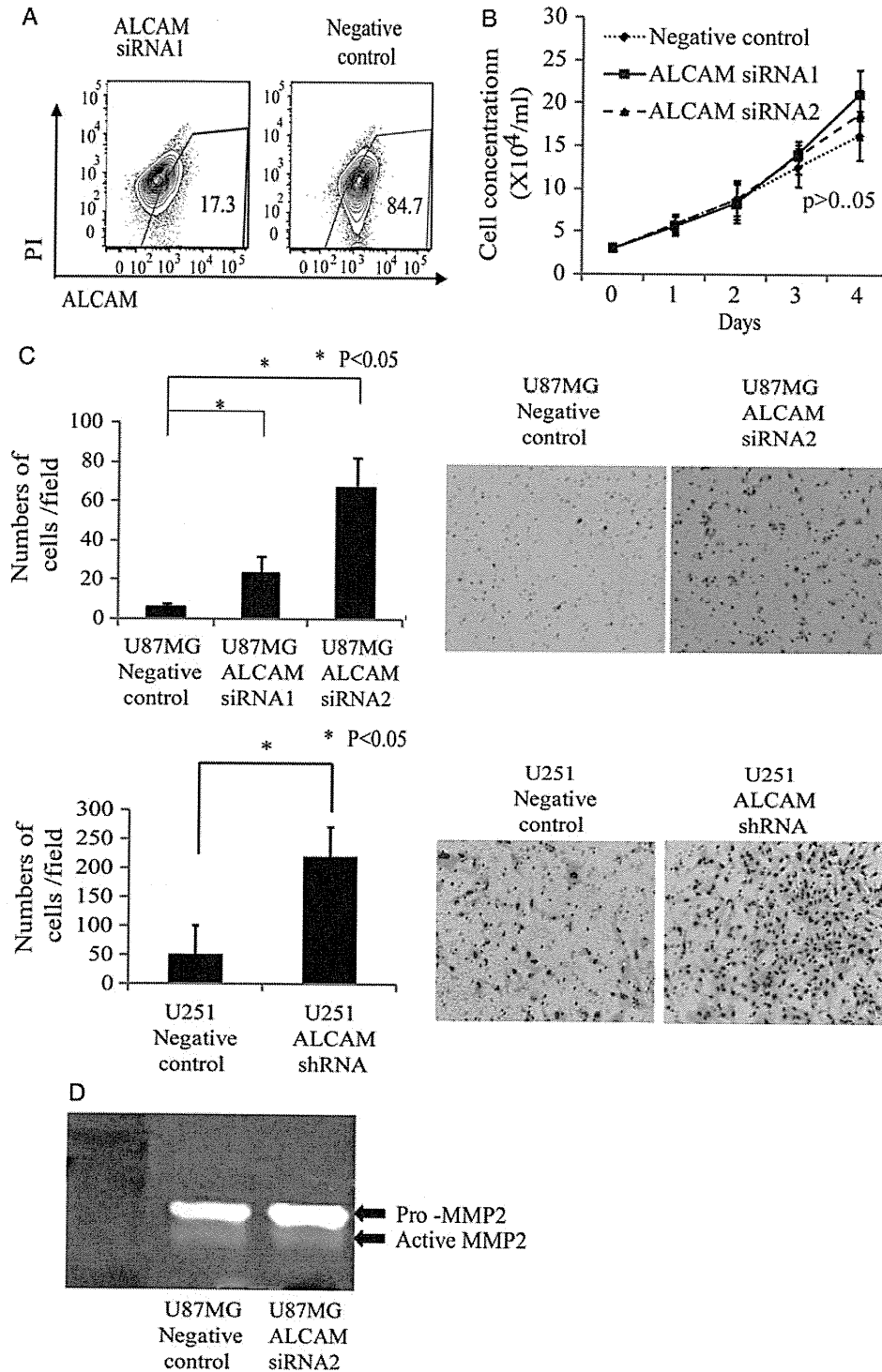


Fig. 3. Downregulation of ALCAM expression on glioblastoma cells promotes cell invasion. (A) FACS analysis of ALCAM expression on anti-ALCAM siRNA-transfected or negative control siRNA-transfected U87MG cells. (B) Comparison of cell proliferation between anti-ALCAM siRNA-transfected and negative control siRNA-transfected U87MG cells. (C) Matrigel invasion assay with anti-ALCAM siRNA-transfected, anti-ALCAM shRNA-transfected, or negative control-transfected U87MG and U251 cells. Bar graph shows numbers of cells having migrated through Matrigel layer. Representative pictures of cells having penetrated to the bottom side of the membrane. (D) Gelatin zymography using medium conditioned by anti-ALCAM siRNA-transfected or negative control siRNA-transfected U87MG cells.

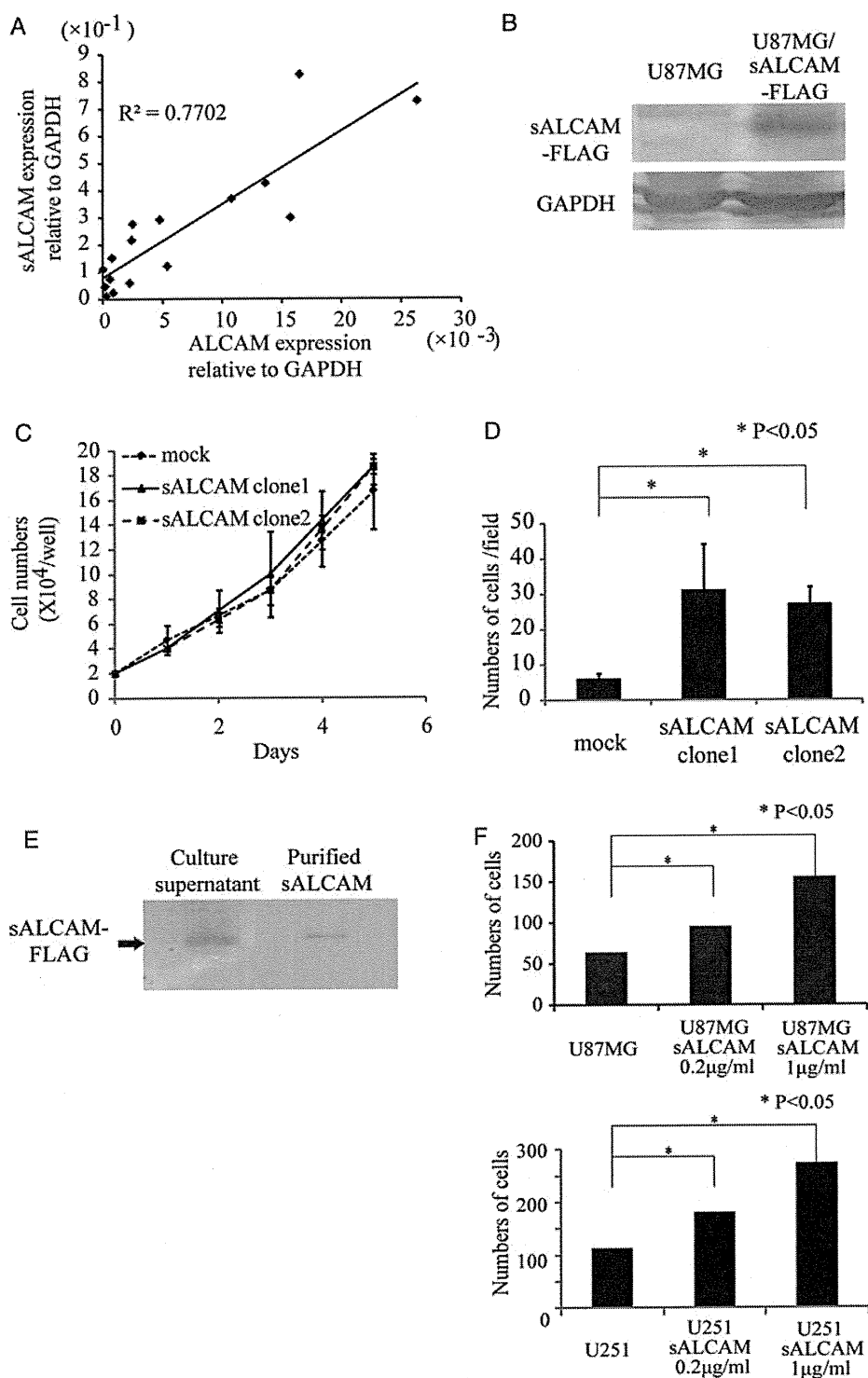


Fig. 4. A soluble isoform of ALCAM is expressed in glioblastoma cells and promotes cell invasion. (A) Correlation between ALCAM mRNA expression and sALCAM mRNA expression in glioblastoma samples. (B) Detection by western blot with anti-FLAG mAb of sALCAM-FLAG protein in cell lysate of sALCAM-expressing U87MG cells. (C) Comparison of cell proliferation between empty vector-transduced U87MG cells (U87MG-mock) and sALCAM-expressing U87MG (U87MG-sALCAM) cells. Two independent clones of U87MG-sALCAM cells were used for the experiments. (D) Matrigel invasion assay with U87MG-mock or U87MG-sALCAM cells. Numbers of cells having passed through the Matrigel layer are shown. (E) Detection by western blot with anti-FLAG mAb of sALCAM-FLAG protein in culture supernatant of U87MG-sALCAM cells and purified sALCAM-FLAG. (F) Matrigel invasion assay with U87MG and U251 cells. Purified sALCAM (0.2 µg/ml, 1 µg/ml) was added to the upper chamber of the transwells.

transplanted with the U87MG-sALCAM cells died of glioblastoma development within 35 days after tumor injection, while none of the mice transplanted with the U87MG-mock cells had developed glioblastoma by posttransplant day 35 (Fig. 5A and B), thus demonstrating that sALCAM significantly enhances tumor progression *in vivo*.

Discussion

In this study we showed that ALCAM⁺ CD133⁺ glioblastoma cells are enriched with tumor sphere-initiating cells, indicating that ALCAM is a novel glioblastoma progenitor cell marker. Some researchers have reported that glioblastoma stem-like cells can be derived from CD133⁻ cells,^{6,36,37} and we also found that some glioblastoma samples contained no CD133⁺ cells. For

such a CD133⁻ glioblastoma sample, ALCAM is also useful for the identification of glioblastoma progenitor cells. Furthermore, immunohistochemical analysis with anti-ALCAM mAb is effective for the identification of glioblastoma progenitor cells in tumor specimens.

While previous studies reported that ALCAM could be used as a prognostic factor for several types of cancers, their conclusions differed. Some studies concluded that high levels of ALCAM expression were related to poor prognosis for breast cancer,³⁸ colorectal cancer,³⁹ pancreatic cancer,⁴⁰ and melanoma.⁴¹ On the other hand, other studies came to the conclusion that high ALCAM expression was a favorable prognostic factor for prostate cancer,⁴² breast cancer,^{43,44} and epithelial ovarian cancer.⁴⁵ This is probably because, as discussed below, the function of ALCAM varies depending on the cell type and the microenvironment surrounding tumor cells. Our results showed that the frequencies of ALCAM⁺ cells in primary glioblastomas correlated significantly with both PFS and OS using an arbitrary cutoff value. We also examined other cutoff values of $\leq 50\%$, but the difference in survival was not significant statistically, which might be due to small patient numbers and/or the difficulties in matching other prognostic factors between the 2 groups. These suggested that the frequency of ALCAM⁺ cells is a candidate prognostic marker for glioblastoma, but its significance needs to be tested in further studies with greater numbers of patients using multivariate analysis.

Knockdown of ALCAM expression in glioblastoma cells resulted in promotion of tumor cell invasion without affecting cell proliferation. This finding is compatible with previously reported results for a metastatic melanoma cell line. In the case of melanoma, interference with endogenous ALCAM by the expression of an amino terminal-truncated ALCAM protein increased cell migration and invasive growth *in vitro*,²⁶ while in a metastatic melanoma cell line, downregulation of ALCAM expression by siRNA inhibited MMP-2 activation.²⁵ However, no such effect on MMP-2 was observed in the glioblastoma cells used in our experiments. The function of ALCAM may thus vary depending on the cell type and/or microenvironment.

Van Kilsdonk et al.²⁸ showed that the soluble isoform of ALCAM attenuated the invasion of melanoma cell lines *in vitro* and also in reconstructed skin. This finding led us to hypothesize that sALCAM also attenuates the invasion of glioblastoma cells, and sALCAM was in fact highly expressed and secreted from glioblastoma cells. However, in contrast to our supposition, overexpression of sALCAM in glioblastoma cells enhanced tumor cell invasion *in vitro* and tumor progression *in vivo*. Another study found that sALCAM also promoted cell migration in endothelial cells *in vitro*.²⁷ The functions of sALCAM may therefore also vary depending on the cell type and microenvironment.

In conclusion, ALCAM is expressed in glioblastoma progenitor cells. Frequencies of ALCAM-expressing cells may correlate with disease progression of glioma and prognosis of glioblastoma patients. Furthermore, we showed that not only membrane-bound ALCAM

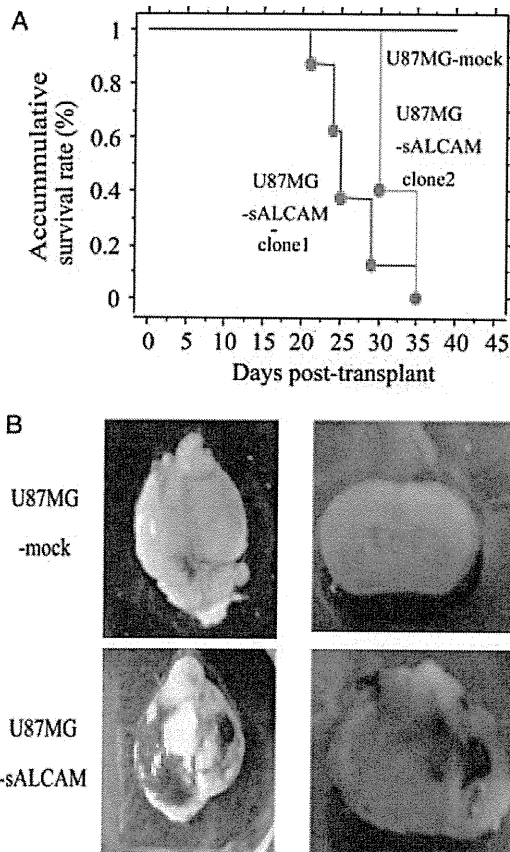


Fig. 5. Expression of sALCAM in U87MG glioblastoma cells promotes tumor progression *in vivo*. (A) Newborn pups of Rag2^{-/-}γc^{-/-} mice were injected with U87MG-sALCAM or U87MG-mock cells. Two independent clones of U87MG-sALCAM cells were used for the experiments. Kaplan-Meier survival curve for each group is shown. (B) Representative photos of the brain of the mouse transplanted with U87MG-sALCAM cells and of the one transplanted with control U87MG cells.

but also sALCAM are involved in the regulation of glioblastoma cell invasion.

Acknowledgments

We wish to thank Tal Raveh, PhD (Stanford University), for valuable technical advice, Irving L. Weissman, MD (Stanford University) for kindly donating Rag2^{-/-}γc^{-/-} mice, Koji Ikeda, MD (Kyoto Prefectural University of Medicine) for kindly donating sALCAM-p3XFLAG, Ms. Mariko Kakinoki (Osaka University) for data collection, and Ms. Mariko Kihara (Osaka University) for technical assistance.

Conflict of interest statement. None declared.

Funding

This work was supported by a grant from the Knowledge Cluster Initiative (Stage II) established by the Ministry of Education, Culture, Sports, Science, and Technology of Japan (to Naoki Hosen) and from the Ministry of Education, Culture, Sports, Science, and Technology of Japan (grant 21591870 to Naoki Kagawa and grant 22791343 to Noriyuki Kijima).

References

- Stupp R, Mason WP, van den Bent MJ, et al. Radiotherapy plus concomitant and adjuvant temozolomide for glioblastoma. *N Engl J Med.* 2005;352:987–996.
- Singh SK, Hawkins C, Clarke ID, et al. Identification of human brain tumour initiating cells. *Nature.* 2004;432:396–401.
- Galli R, Binda E, Orfanelli U, et al. Isolation and characterization of tumorigenic, stem-like neural precursors from human glioblastoma. *Cancer Res.* 2004;64:7011–7021.
- Bao S, Wu Q, McLendon RE, et al. Glioma stem cells promote radioresistance by preferential activation of the DNA damage response. *Nature.* 2006;444:756–760.
- Son MJ, Woolard K, Nam DH, Lee J, Fine HA. SSEA-1 is an enrichment marker for tumor-initiating cells in human glioblastoma. *Cell Stem Cell.* 2009;4:440–452.
- Ogden AT, Waziri AE, Lochhead RA, et al. Identification of A2B5+CD133- tumor-initiating cells in adult human gliomas. *Neurosurgery.* 2008;62:505–514. discussion 14–5.
- Bao S, Wu Q, Li Z, et al. Targeting cancer stem cells through L1CAM suppresses glioma growth. *Cancer Res.* 2008;68:6043–6048.
- Lathia JD, Gallagher J, Heddleston JM, et al. Integrin alpha 6 regulates glioblastoma stem cells. *Cell Stem Cell.* 2010;6:421–432.
- Teodorczyk M, Martin-Villalba A. Sensing invasion: cell surface receptors driving spreading of glioblastoma. *J Cell Physiol.* 2010;222:1–10.
- Perego C, Vanoni C, Massari S, et al. Invasive behaviour of glioblastoma cell lines is associated with altered organisation of the cadherin-catenin adhesion system. *J Cell Sci.* 2002;115:3331–3340.
- Owens GC, Orr EA, DeMasters BK, Muschel RJ, Berens ME, Kruse CA. Overexpression of a transmembrane isoform of neural cell adhesion molecule alters the invasiveness of rat CNS-1 glioma. *Cancer Res.* 1998;58:2020–2028.
- Fukushima Y, Ohnishi T, Arita N, Hayakawa T, Sekiguchi K. Integrin alpha3beta1-mediated interaction with laminin-5 stimulates adhesion, migration and invasion of malignant glioma cells. *Int J Cancer.* 1998;76:63–72.
- Tanaka H, Matsui T, Agata A, et al. Molecular cloning and expression of a novel adhesion molecule, SC1. *Neuron.* 1991;7:535–545.
- Johnston IG, Paladino T, Gurd JW, Brown IR. Molecular cloning of SC1: a putative brain extracellular matrix glycoprotein showing partial similarity to osteonectin/BM40/SPARC. *Neuron.* 1990;4:165–176.
- Burns FR, von Kannen S, Guy L, Raper JA, Kamholz J, Chang S. DM-GRASP, a novel immunoglobulin superfamily axonal surface protein that supports neurite extension. *Neuron.* 1991;7:209–220.
- Ohneda O, Ohneda K, Arai F, et al. ALCAM (CD166): its role in hematopoietic and endothelial development. *Blood.* 2001;98:2134–2142.
- Cayrol R, Wosik K, Berard JL, et al. Activated leukocyte cell adhesion molecule promotes leukocyte trafficking into the central nervous system. *Nat Immunol.* 2008;9:137–145.
- Nakamura Y, Arai F, Iwasaki H, et al. Isolation and characterization of endosteal niche cell populations that regulate hematopoietic stem cells. *Blood.* 2010;116:1422–1432.
- Pittenger MF, Mackay AM, Beck SC, et al. Multilineage potential of adult human mesenchymal stem cells. *Science.* 1999;284:143–147.
- Bruder SP, Ricalton NS, Boynton RE, et al. Mesenchymal stem cell surface antigen SB-10 corresponds to activated leukocyte cell adhesion molecule and is involved in osteogenic differentiation. *J Bone Miner Res.* 1998;13:655–663.
- Uchida N, Yang Z, Combs J, et al. The characterization, molecular cloning, and expression of a novel hematopoietic cell antigen from CD34+ human bone marrow cells. *Blood.* 1997;89:2706–2716.
- Dalerba P, Dylla SJ, Park IK, et al. Phenotypic characterization of human colorectal cancer stem cells. *Proc Natl Acad Sci USA.* 2007;104:10158–10163.
- Rajasekhar VK, Studer L, Gerald W, Socci ND, Scher HI. Tumour-initiating stem-like cells in human prostate cancer exhibit increased NF-kappaB signalling. *Nat Commun.* 2011;2:162.
- Ofori-Acquah SF, King JA. Activated leukocyte cell adhesion molecule: a new paradox in cancer. *Transl Res.* 2008;151:122–128.
- Lunter PC, van Kilsdonk JW, van Beek H, et al. Activated leukocyte cell adhesion molecule (ALCAM/CD166/MEMD), a novel actor in invasive growth, controls matrix metalloproteinase activity. *Cancer Res.* 2005;65:8801–8808.
- van Kempen LC, Meier F, Egeblad M, et al. Truncation of activated leukocyte cell adhesion molecule: a gateway to melanoma metastasis. *J Invest Dermatol.* 2004;122:1293–1301.
- Ikeda K, Quertermous T. Molecular isolation and characterization of a soluble isoform of activated leukocyte cell adhesion molecule that modulates endothelial cell function. *J Biol Chem.* 2004;279:55315–55323.
- van Kilsdonk JW, Wilting RH, Bergers M, et al. Attenuation of melanoma invasion by a secreted variant of activated leukocyte cell adhesion molecule. *Cancer Res.* 2008;68:3671–3679.

29. Albini A, Iwamoto Y, Kleinman HK, et al. A rapid in vitro assay for quantitating the invasive potential of tumor cells. *Cancer Res.* 1987;47:3239–3245.
30. Yan H, Parsons DW, Jin G, et al. IDH1 and IDH2 mutations in gliomas. *N Engl J Med.* 2009;360:765–773.
31. Parsons DW, Jones S, Zhang X, et al. An integrated genomic analysis of human glioblastoma multiforme. *Science.* 2008;321:1807–1812.
32. Ichimura K, Pearson DM, Kocialkowski S, et al. IDH1 mutations are present in the majority of common adult gliomas but rare in primary glioblastomas. *Neuro Oncol.* 2009;11:341–347.
33. Nobusawa SWT, Kleihues P, Ohgaki H. IDH1 mutations as molecular signature and predictive factor of secondary glioblastomas. *Clin Cancer Res.* 2009;15:6002–6007.
34. Mellai MPA, Caldera V, Monzeglio O, Cassoni P, Valente G, Schiffer D. IDH1 and IDH2 mutations, immunohistochemistry and associations in a series of brain tumors. *J Neurooncol.* 2011;105(2):345–357.
35. Preusser M, Wohrer A, Stary S, et al. Value and Limitations of Immunohistochemistry and Gene Sequencing for Detection of the IDH1-R132H Mutation in Diffuse Glioma Biopsy Specimens. *J Neuropathol Exp Neurol.* 2011;70:715–723.
36. Beier D, Hau P, Proescholdt M, et al. CD133(+) and CD133(-) glioblastoma-derived cancer stem cells show differential growth characteristics and molecular profiles. *Cancer Res.* 2007;67:4010–4015.
37. Wang J, Sakariassen PO, Tsinkalovsky O, et al. CD133 negative glioma cells form tumors in nude rats and give rise to CD133 positive cells. *Int J Cancer.* 2008;122:761–768.
38. Burkhardt M, Mayordomo E, Winzer KJ, et al. Cytoplasmic overexpression of ALCAM is prognostic of disease progression in breast cancer. *J Clin Pathol.* 2006;59:403–409.
39. Weichert W, Knosel T, Bellach J, Dietel M, Kristiansen G. ALCAM/CD166 is overexpressed in colorectal carcinoma and correlates with shortened patient survival. *J Clin Pathol.* 2004;57:1160–1164.
40. Kahler C, Weber H, Mogler C, et al. Increased expression of ALCAM/CD166 in pancreatic cancer is an independent prognostic marker for poor survival and early tumour relapse. *Br J Cancer.* 2009;101:457–464.
41. van Kempen LC, van den Oord JJ, van Muijen GN, Weidle UH, Bloemers HP, Swart GW. Activated leukocyte cell adhesion molecule/CD166, a marker of tumor progression in primary malignant melanoma of the skin. *Am J Pathol.* 2000;156:769–774.
42. Kristiansen G, Pilarsky C, Wissmann C, et al. ALCAM/CD166 is up-regulated in low-grade prostate cancer and progressively lost in high-grade lesions. *Prostate.* 2003;54:34–43.
43. King JA, Ofori-Acquah SF, Stevens T, Al-Mehdi AB, Fodstad O, Jiang WG. Activated leukocyte cell adhesion molecule in breast cancer: prognostic indicator. *Breast Cancer Res.* 2004;6:R478–R487.
44. Ihnen M, Muller V, Wirtz RM, et al. Predictive impact of activated leukocyte cell adhesion molecule (ALCAM/CD166) in breast cancer. *Breast Cancer Res Treat.* 2008;112:419–427.
45. Mezzanzanica D, Fabbi M, Bagnoli M, et al. Subcellular localization of activated leukocyte cell adhesion molecule is a molecular predictor of survival in ovarian carcinoma patients. *Clin Cancer Res.* 2008;14:1726–1733.

Biased usage of T cell receptor β -chain variable region genes of Wilms' tumor gene (WT1)-specific CD8⁺ T cells in patients with solid tumors and healthy donors

Soyoko Morimoto,¹ Yoshihiro Oka,¹ Akihiro Tsuboi,² Yukie Tanaka,³ Fumihiko Fujiki,⁴ Hiroko Nakajima,⁴ Naoki Hosen,⁵ Sumiyuki Nishida,² Jun Nakata,¹ Yoshiki Nakae,¹ Motohiko Maruno,⁶ Akira Myoui,⁷ Takayuki Enomoto,⁸ Shuichi Izumoto,⁹ Mitsugu Sekimoto,¹⁰ Naoki Kagawa,¹¹ Naoya Hashimoto,¹¹ Toshiki Yoshimine,¹¹ Yusuke Oji,¹² Atsushi Kumanogoh¹ and Haruo Sugiyama^{5,13}

Departments of ¹Respiratory Medicine, Allergy and Rheumatic Diseases, ²Cancer Immunotherapy, Osaka University Graduate School of Medicine, Osaka; ³Division of Hematology, Saitama Medical Center, Jichi Medical University, Saitama; Departments of ⁴Cancer Immunology, ⁵Functional Diagnostic Science, Osaka University Graduate School of Medicine, Osaka; ⁶Department of Neurosurgery, Osaka Medical Center for Cancer and Cardiovascular Diseases, Osaka; ⁷Medical Center for Translational Research, Osaka University Hospital, Osaka; ⁸Department of Obstetrics and Gynecology, Osaka University Graduate School of Medicine, Osaka; ⁹Department of Neurosurgery, Hyogo College of Medicine, Hyogo; Departments of ¹⁰Gastroenterological Surgery, ¹¹Neurosurgery, ¹²Cancer Stem Cell Biology, Osaka University Graduate School of Medicine, Osaka, Japan

(Received July 7, 2011/Revised November 15, 2011/Accepted November 21, 2011/Accepted manuscript online November 29, 2011/Article first published online January 17, 2012)

Wilms' tumor gene 1 (WT1) protein is a promising tumor-associated antigen. In patients with WT1-expressing malignancies, WT1-specific CTLs are spontaneously induced as a result of an immune response to the WT1 protein. In the present study, we performed single cell-level comparative analysis of T cell receptor β -chain variable region (TCR-BV) gene families of a total of 750 spontaneously induced WT1₁₂₆ peptide (amino acids 126–134, WT1₁₂₆)-specific CTLs in both HLA-A*0201⁺ patients with solid tumors and healthy donors (HDs). This is the first report of direct usage analysis of 24 kinds of TCR-BV gene families of WT1₁₂₆-specific CTLs at the single cell level. Usage analysis with single-cell RT-PCR of TCR-BV gene families of individual FACS-sorted WT1₁₂₆ tetramer⁺ CD8⁺ T cells showed, for the first time, that: (i) BVs 3, 6, 7, 20, 27, and 28 were commonly biased in patients and HDs; (ii) BVs 2, 11, and 15 were biased only in patients; and (iii) BVs 4, 5, 9, and 19 were biased only in HDs. However, statistical analysis of similarity of individual usage frequencies of 24 kinds of TCR-BV gene families between patients and HDs indicated that the usage frequencies of TCR-BV gene families in patients reflected those in HDs. These results should provide us with a novel insight for a better understanding of WT1-specific immune responses. (*Cancer Sci* 2012; 103: 408–414)

Wilms' tumor gene (*WT1*) encodes a zinc-finger transcription factor and plays important roles in the regulation of cell proliferation, differentiation, and apoptosis.^(1–3) The *WT1* gene was originally isolated as the gene responsible for a childhood renal neoplasm, namely Wilms' tumor, and was first categorized as a tumor-suppressor gene.^(4,5) However, based on the result of a series of studies,^(6–8) we proposed that the wild-type *WT1* gene had an oncogenic rather than a tumor-suppressor function in various kinds of hematological malignancies and solid tumors. Indeed, the *WT1* gene is expressed at high levels in acute myeloid leukemia (AML), acute lymphocytic leukemia, chronic myelogenous leukemia, and myelodysplastic syndromes (MDS), as well as in various types of solid tumors.^(9–14) Because a correlation has been shown between *WT1* mRNA transcript levels and the amount of minimal residual disease (MRD) in the peripheral blood (PB) or bone marrow of leukemia patients,^(15–17) measurement of *WT1* mRNA transcripts is now being used to monitor MRD in leukemia patients.

Previous studies have reported that WT1-specific CTLs can be generated from human PBMC in a human leukocyte antigen (HLA) Class I-restricted manner and can lyse WT1-expressing tumor cells as well as WT1 peptide-pulsed target cells.^(18,19) Mice immunized with WT1 peptide or WT1 plasmid DNA elicit WT1-specific CTLs and reject challenges by WT1-expressing tumor cells.^(20,21) Furthermore, WT1-specific CTLs and antibodies are induced spontaneously in WT1-expressing tumor-bearing patients.^(22–24) These results indicate that the WT1 protein is highly immunogenic and a promising target antigen for cancer immunotherapy. In fact, WT1 has been rated as the most promising cancer antigen of 75 tumor-associated antigens.⁽²⁵⁾

On the basis of the results of these preclinical studies, clinical studies of WT1 peptide vaccination were undertaken,^(26–29) with promising clinical effects, including a reduction in leukemic blast cells and tumor size, as well as long-term stable disease, being seen in association with an increase in the frequency of WT1-specific CD8⁺ T cells in PB.^(26,27) In this context, analysis of the clonality of the WT1-specific CTLs is important to gain a better understanding of the WT1-specific CTL response in WT1-expressing tumor-bearing patients and, further, to obtain clues as to how to enhance WT1-specific CTL responses in WT1 immunotherapy.

Recently, using single-cell RT-PCR analysis of the T cell receptor β -chain variable region (TCR-BV) genes of individual FACS-sorted WT1 tetramer⁺ CD8⁺ T cells, we demonstrated biased usage of TCR-BV gene families of WT1₂₃₅ peptide (amino acids 235–243)-specific CTLs in HLA-A*2402⁺ patients with AML or MDS, which reflected the biased usage in healthy donors (HDs).⁽³⁰⁾

In the present study, we examined usage frequencies of TCR-BV gene families of CTLs specific for WT1₁₂₆, an HLA-A*0201-restricted CTL epitope, in both patients with solid tumors and HDs and found biased usage for these TCR-BV gene families in both the patients and HDs and that the patterns of biased usage were very similar between the two groups.

¹³To whom correspondence should be addressed.
E-mail: sugiyama@sahs.med.osaka-u.ac.jp

Table 1. Characteristics of the patients and healthy donors

	Gender	Age (years)	Disease	Clinical stage	Prior therapy
Patients					
PT-1	M	33	GBM	N/A	Ope/RT
PT-2	F	56	GBM	N/A	Ope/RT
PT-3	M	28	GBM	N/A	Ope/RT/Chemo
PT-4	M	18	PNET	IV	Ope/RT/Chemo/ auto-PBSCT
PT-5	F	53	Ovarian cancer	IIIc	Ope/Chemo
PT-6	F	73	Cecal cancer	IV	Ope/Chemo
Healthy donors					
HD-1	F	23			
HD-2	M	45			
HD-3	F	24			
HD-4	F	25			
HD-5	M	37			

auto-PBSCT, autologous peripheral blood stem cell transplantation; Chemo, chemotherapy; GBM, glioblastoma multiforme; N/A, not available; Ope, operation; PNET, primitive neuroectodermal tumor; RT, radiation therapy.

Materials and Methods

Samples of PB from patients with solid tumors and HDs. Analysis of WT1₁₂₆-specific CTLs in PBMC was approved by the Institutional Review Board for Clinical Research, Osaka University Hospital. After written informed consent had been obtained, PB samples were obtained from six HLA-A*0201⁺ patients with a solid tumor (patient (PT)-1, -2, -3, -4, -5, and -6) and five HLA-A*0201⁺ HDs. Expression of WT1 protein in tumor cells was determined by immunohistochemical analysis, as described elsewhere.⁽³¹⁾ The PBMC were separated by density gradient centrifugation using Ficoll-Hypaque (Pharmacia, Uppsala, Sweden) and cryopreserved in liquid nitrogen until use. Table 1 summarizes the characteristics of both the patients and HDs.

Flow cytometric analysis and single-cell sorting of WT1 tetramer⁺ CD8⁺ T cells. Thawed PBMC were rested at 37°C for 1.5 h in RPMI 1640 containing 10% FBS before being stained with phycoerythrin (PE)-labeled HLA-A*0201/WT1₁₂₆ tetramer (WT1₁₂₆ tetramer; MBL, Tokyo, Japan) in FACS buffer composed of PBS containing 5% FBS at 37°C for 30 min. The PBMC were then stained with a panel of mAbs at 4°C for 25 min in the dark, washed three times with FACS buffer, and finally resuspended in appropriate quantities of FACS buffer. The following mAbs were used: anti-CD4-FITC, anti-CD16-FITC, anti-CD45RA-allophycocyanin (APC) (BioLegend, San

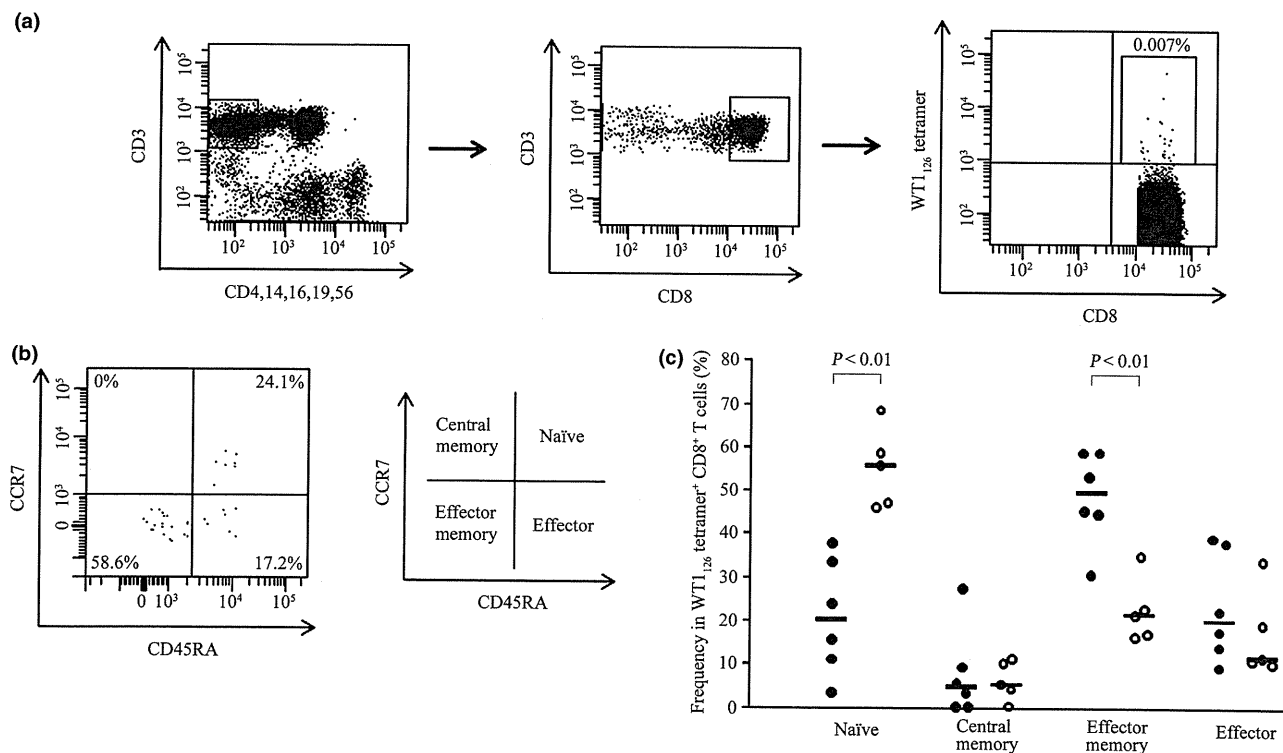


Fig. 1. Frequencies of WT1₁₂₆ tetramer⁺ CD8⁺ T cells in peripheral blood of patients with a solid tumor and healthy donors and phenotypic analysis of WT1₁₂₆ tetramer⁺ CD8⁺ T cells. (a) Representative data of flow cytometric analysis using WT1₁₂₆ tetramer. CD4⁻, CD14⁻, CD16⁻, CD19⁻, CD56⁻, and WT1₁₂₆ tetramer⁺ CD8⁺ T cells were defined as WT1₁₂₆ tetramer⁺ CD8⁺ T cells. The percentages shown represent the frequencies of WT1₁₂₆ tetramer⁺ CD8⁺ T cells among total CD3⁺ CD8⁺ T cells. (b) WT1₁₂₆ tetramer⁺ CD8⁺ T cells were classified into four distinct differentiation stages according to the cell surface expression of CCR7 and CD45RA as follows: (i) CCR7⁺ CD45RA⁺ (naïve) cells; (ii) CCR7⁺ CD45RA⁻ (central memory) cells; (iii) CCR7⁻ CD45RA⁻ (effector memory) cells; and (iv) CCR7⁻ CD45RA⁺ (effector) cells. Representative data from Patient 3 are shown. (c) Frequencies of each subset of WT1₁₂₆ tetramer⁺ CD8⁺ T cells. Closed and open circles represent patients and healthy donors, respectively. Bars indicate the median values of the frequencies.